DIAGNOSIS OF BRAIN TUMOUR WITH CT IMAGES USING NEURO FUZZY CLASSIFIER

PROJECT REPORT

Submitted by

VINOTH RAMANAN R

Register No: 13MAE18

in partial fulfillment for the requirement of award of the degree

of

MASTER OF ENGINEERING

in

APPLIED ELECTRONICS

Department of Electronics and Communication Engineering

KUMARAGURU COLLEGE OF TECHNOLOGY
(An Autonomous Institution affiliated to Anna University, Chennai)

COIMBATORE - 641049

ANNA UNIVERSITY: CHENNAI 600 025

APRIL -2015

BONAFIDE CERTIFICATE

Certified that this project report titled **"DIAGNOSIS OF BRAIN TUMOUR WITH CT IMAGES USING NEURO FUZZY CLASSIFIER"** is the bonafide work of **VINOTH RAMANAN.R [Reg. No. 13MAE18]** who carried out the research under my supervision. Certified further, that to the best of my knowledge the work reported herein does not form part of any other project or dissertation on the basis of which a degree or award was conferred on an earlier occasion on this or any other candidate.

SIGNATURE   **SIGNATURE**

Ms.M.ALAGUMEENAAKSHI   **Dr. RAJESWARI MARIAPPAN**

PROJECT SUPERVISOR   **HEAD OF THE DEPARTMENT**

Department of ECE   Department of ECE

Kumaraguru College of Technology   Kumaraguru College of Technology

Coimbatore-641 049   Coimbatore-641 049

The Candidate with **Register No. 13MAE18** was examined by us in the project viva –voice examination held on...

INTERNAL EXAMINER   **EXTERNAL EXAMINER**

ACKNOWLEDGEMENT

First, I would like to express my praise and gratitude to the Lord, who has showered his grace and blessing enabling me to complete this project in an excellent manner.

I express my sincere thanks to the management of Kumaraguru College of Technology and Joint Correspondent **Shri. Shankar Vanavarayar** for the kind support and for providing necessary facilities to carry out the work.

I would like to express my sincere thanks to our beloved Principal **Dr.R.S.Kumar Ph.D.,** Kumaraguru College of Technology, who encouraged me in each and every steps of the project.

I would like to thank **Dr. Rajeswari Mariappan Ph.D.,** Head of the Department, Electronics and Communication Engineering, for her kind support and for providing necessary facilities to carry out the project work.

In particular, I wish to thanks with everlasting gratitude to the Project Coordinator **Ms.S.Sasikala M.Tech.,** Associate Professor, Department of Electronics and Communication for her expert counseling and guidance to make this project to a great deal of success.

I am greatly privileged to express my heartfelt thanks to my guide **Ms.M.Alagumeenaakshi M.E(Ph.D).,** Assistant Professor(SRG), Department of Electronics and Communication Engineering, throughout the course of this project work and I wish to convey my deep sense of gratitude to all teaching and non- teaching staff members of ECE department for their help and cooperation.

Finally I thank my parents and my family members for giving me the moral support and abundant blessings in all of my activities and my dear friends who helped me to endure my difficult times with their unfailing support and warm wishes.

ABSTRACT

Computed Tomography (CT) images are usually corrupted by several noises from the measurement process complicating the automatic feature extraction and analysis of clinical data. To attain the best possible diagnosis it is very vital that medical images be clear, sharp, and free of noise and artifacts. In this project, proposed a robust technique to denoise, detect and classify the tumour part from CT medical images. The proposed approach consists of four phases, such as Image denoising, Region segmentation, Feature extraction and Classification. In the denoising phase Curvelet Transform is used in order to remove the noise and it will not affect the lower dimensions. Here using the Rician noise for proposed denoising technique. The performance of this technique is assessed on the six CT images for the parameter, PSNR. In the segmentation process K-means clustering technique is employed. For the feature extraction, the following parameters such as contrast, correlation, energy and homogeneity are extracted. In classification, a modified technique called Adaptive Neuro Fuzzy Inference system (ANFIS) algorithm is developed and applied for detection of the tumour region.

TABLE OF CONTENTS

LIST OF TABLES

LIST OF FIGURES

LIST OF ABBREVIATIONS

ACRONYMS	ABBREVIATIONS
CT	Computed Tomography
K-NN	K-means Neural Network
SPECT	Single Photon Emission Computed Tomography
PET	Photon Emission Tomography
PSNR	Peak Signal to Noise Ratio
ANFIS	Adaptive Neuro Fuzzy Inference System
GLCM	Gray Level Co-occurrence Matrix
SAR	Synthetic Aperture Radar
MSE	Mean Squared Error
2-D FFT	2-Dimensional Fast Fourier Transform
1-D IFFT	1-Dimensional Inverse Fast Fourier Transform
PSNR	Peak Signal to Noise Ratio
SDME	Second Derivative Measure of Enhancement
MRF	Markov Random Field
RKM	Region K level Means
MIRGS	Multivariate Iterative Region Growing using Semantics
DWT	Discrete Wavelet Transform
MSE	Mean Squared Error
FCM	Fuzzy C-means
LSE	Least Squared Error
SWT	Single Wavelet Transform
3-D	3 Dimensional

PET	Positron Emission Tomography
MRI	Magnetic Resonance Imaging
GVF	Gradient Vector Flow
MAC	Magnetostatic Active Contour
EMD	Empirical Mode Decomposition
RDTDWT	Real Dual Tree Discrete Wavelet Transform
ISNN	Incremental Supervised Neural Network
CWT	Continuous Wavelet Transform
IRGS	Iterative Region Growing using Semantics
RAM	Random Access Memory
GB	Giga Bytes
JPEG	Joint Photographic Expert Group
DTCWP	Dual Tree Complex Wavelet Packet
CLAHE	Contrast Limited Adaptive Histogram Equalization

CHAPTER-1

INTRODUCTION

1. CT IMAGE OVERVIEW:

Denoising of medical images like X-RAY, CT is encompass diminutive information about heart, brain, nerves and more which leads physician for precise analysis of diseases. In the case of CT, numerous mathematical and medical applications can be applied to conclude whether the normal tissue has been infected by the mutations of the cancer cell. Recent wavelet thresholding based denoising methods have proved capable, during the conservation of the high frequency signal details. The threshold at certain scale is a constant for all wavelet coefficients in standard wavelet thresholding based noise reduction methods. Fundamentally, the noisy image is transformed into the wavelet domain, then the wavelet coefficients are shifted to soft or hard thresholding, and the result has been inverse transformed in the final step. Medical image segmentation casts an amazing part in the treatment planning, identifying tumors, tumor volume, patient follow up and computer guided surgery. There is a flood of varied methods for performing the function of medical image segmentation. Feature extraction is the task of mining definite features from the pre-processed image.

A number of experimenters have launched associated investigations into K-means clustering segmentation. Though a significant and noteworthy advancement has been made in this regard, still there is greater computational intricacy and the need for superfluous software functionality. Clustering programs, like k-means function in an unsupervised mode and have been performed on an extensive domain of categorization dilemmas.

For categorizing the tumor segments, physical classification tends to lead to manual flaws, in addition to relying heavily on person to person, protracted and elongated runtime along with non-reproducible outcomes. Therefore, an automatic or semi-automatic classification technique is the need of the hour as it tends to scale down the burden on the individual spectator, and also because accuracy does not become the casualty on account of exhaustion and mammoth quantity of images. In respect of tumor detection, several schemes such as, K-NN, bayesian classifier, neural network, fuzzy classifier are performed for automatic detection.

1.1 DIFFERENT TYPES OF NOISES

Noise is undesired information that degrades the image. In the image de-noising process, information of the type of noise present in the original image plays a significant role. Mostly images can be corrupted with noise modeled with either a uniform, Gaussian, or salt and pepper distribution. Another type of noise is a speckle noise which is multiplicative in nature. Noise is present in image either in an additive or multiplicative form.

Rule for additive noise

$$w(x, y) = s(x, y) + n(x, y) , \qquad \ldots\ldots\ldots\ldots \qquad (1)$$

Rule for multiplicative noise

$$w(x, y) = s(x, y) \times n(x, y) , \qquad \ldots\ldots\ldots\ldots \qquad (2)$$

where (x, y) is original signal, $n(x, y)$ is the noise introduced into the signal to produce a noisy image $w(x, y)$, and (x, y) is the pixel location. The above image algebra is done at pixel level. Image addition also has applications in image morphing. Image multiplication means the brightness of the image is varied.

The digital image acquisition process transforms an optical image into a continuous electrical signal that is, sampled. In every step of the process there are fluctuations caused by natural phenomena, adding random value to the exact brightness value for a given pixel.

1.1.1 Gaussian Noise

A gaussian noise is evenly distributed in the signal. That means every pixel in the noisy image is the sum of the random Gaussian distributed noise value and true pixel value. This type of noise has a Gaussian distribution, which has a probability distribution function given by

$$F(g) = \frac{1}{\sqrt{2\pi\sigma^2}} e^{-(g-m)^2} \Big/ 2\sigma^2 \quad \text{.......... (3)}$$

where g represents the gray level, *m* is the mean of the function and σ is standard deviation in the noise. Graphically, it is represented as shown in Figure below.
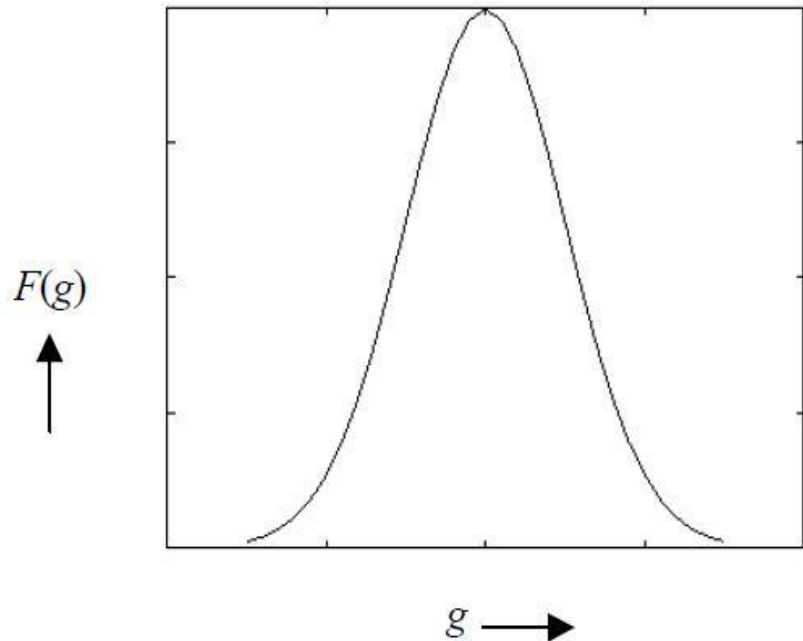
Fig 1.1.1 Gaussian distribution

1.1.2 Salt and Pepper Noise

Salt and pepper noise is impulse type of noise, that is also referred to as intensity spikes. It is caused generally due to the errors in the data transmission. It has only two possible values that is *a* and *b*.

The probability of each is typically less than 0.1. Corrupted pixels can be set alternatively to the minimum or to the maximum value, giving image a "salt and pepper" like appearance. Pixels remain unchanged for unaffected. For a 8-bit image, the value of pepper noise is 0 and for salt noise 255. Salt and pepper noise is mainly caused by malfunctioning of pixel elements in the sensors of cameras, faulty memory locations, or timing errors of the digitization process.

The probability density function for this type of noise is shown in the Figure below.
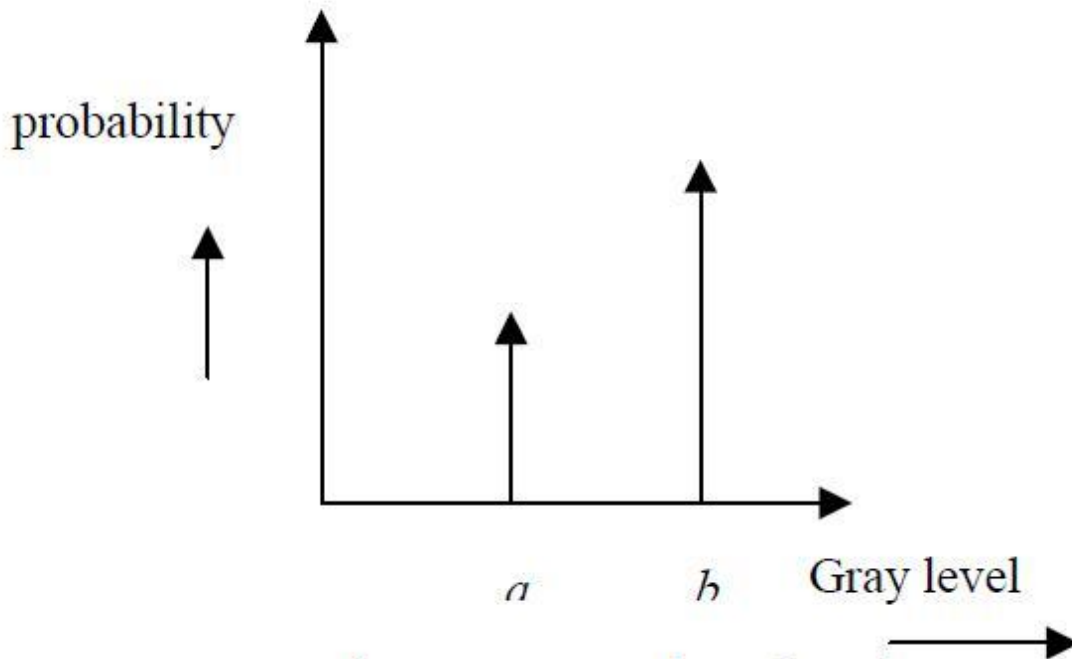
Fig 1.1.2 PDF for salt and pepper noise

1.1.3 Speckle Noise

Speckle noise is multiplicative noise. This type of noise occurs mostly in all coherent imaging systems such as acoustics, laser, acoustics and SAR (Synthetic Aperture Radar) imagery. Source of this noise is attributed to the random interference between the coherent returns. A fully developed speckle noise has the characteristic of multiplicative noise. Speckle noise follows a gamma distribution and given as

$$F(g) = \frac{g^{\alpha-1}}{(\alpha-1)!a^{\alpha}} e^{\frac{-g}{a}} \quad \ldots\ldots\ldots\ldots\ldots(4)$$

where variance is $a^2\alpha$ and g is the gray level.

1.1.4 Poisson Noise

Many images like as those from radiography, have noise that satisfies a poisson distribution. Magnitude of Poisson noise varies across an image and it depends on the image intensity, that makes removing such noise very hard. Poisson images occur in situations where the image acquisition is performed using the detection of particles (e.g) counting photons being emitted from a radioactive source is applied in medical imaging like SPECT and PET , therefore Poisson noise reduction is an essential problem. Poisson noise is generated from the data in place of adding artificial noise to the data. For ex. if a pixel in an unsigned integer input has the value 10, then corresponding output pixel will be generated from Poisson distribution with a mean 10.

1.1.5 Rician Noise

Rician noise is signal dependent and hence it is not a additive noise. It has Rician distributed over the image with the given probability density function,

$$f(x) = \left\{ \frac{x}{\sigma^2} I_0\left(\frac{mx}{\sigma^2}\right) \exp\left(-\frac{x^2 + m^2}{2\sigma^2}\right) x \geq 0 \right.$$

where,

σ is the standard deviation

$m^2 = mI^2 + mQ^2$, where mI and mQ are the mean values of two independent Gaussian components.

I_0 is the modified 0th order Bessel function.

$$I_o(y) = \frac{1}{2\pi} \int_{-\pi}^{\pi} e^{y\cos t} dt$$

1.2 FILTER TYPE

1.2.1 Switching Bilateral Filter

A Switching Bilateral filter is a non-linear, edge-preserving and noise-reducing smoothing filter for images. The intensity value at each pixel in an image is replaced by a weighted average of intensity values from nearby pixels. This weight can be based on a Gaussian distribution. Crucially, the weights depend not only on Euclidean distance of pixels, but also on the radiometric differences (e.g. range differences, such as color intensity, depth distance, etc.). This preserves sharp edges by systematically looping through each pixel and adjusting weights to the adjacent pixels accordingly.

It is defined as,

$$\mathbf{I}^{filtered}(x) = \frac{1}{Wp} \sum_{X_i \in \Omega} I(x_i) f_r(\|I(x_i) - I(x)\|) g_s(\|x_i - x\|)$$

where the normalization term,

$$Wp = \frac{1}{Wp} \sum_{X_i \in \Omega} f_r(\|I(x_i) - I(x)\|) g_s(\|x_i - x\|)$$

ensures that the filter preserves image energy and as follows:

- ➢ $I^{filtered}$ is the filtered image;
- ➢ I is the original input image to be filtered;
- ➢ x are the coordinates of the current pixel to be filtered;
- ➢ Ω is the window centered in x;
- ➢ f_r is the range kernel for smoothing differences in intensities. This function can be a Gaussian function;
- ➢ g_s is the spatial kernel for smoothing differences in coordinates. This function can be a Gaussian function.

1.3 OBJECTIVE OF THE PROJECT

- ➢ To remove the noise in a CT image by Curvelet Transform and its features.
- ➢ To improve the PSNR evaluation.
- ➢ To evaluate the features of the image using feature extraction.
- ➢ To diagnose the brain tumour in CT image with Classification by the Adaptive Neuro Fuzzy Inference System (ANFIS) Classifier.

CHAPTER-2

LITERATURE REVIEW

2.1 PAPERS RELATED TO CT IMAGE DENOISING

Nidhi Chandrakar (2013) has presented a hybrid denoising model is designed through hybridization and its performance is tested on different types of noisy images. Comparison of the results is drawn along with other three methods using established wavelet and bilateral based filtering techniques. It is also observed that the application of bilateral filters on wavelet decomposed subbands in any combination with wavelet thresholding deteriorates the performance of the model, whereas, the application of bilateral filters on both before and after decomposition enhances the performance.

Anja Borsdorf (2008) has presented the wavelet domain denoising technique for the suppression of pixel noise in CT (Computed Tomography) images. The separate reconstruction from disjoint subsets of projections allows the generation of images which only differ with respect to image noise but include the same information. He showed that correlation analysis based on the detail coefficients of the á-trous wavelet decomposition of the input images, as recently proposed by Tischenko, allows the separation of structures and noise, without assuming or estimating the underlying noise distribution. They extended the approach for the applicability with DWT (Dyadic Wavelet Transformation) and SWT (Stationary Wavelet Transformation).

Guangming Zhang (2010) has presented a statistical technique where the goal is to represent a set of random variables as a linear transformation of statistically independent component variables. The curvelet transform as a multiscale transform has directional parameters occurs at all scales, locations, and orientations. This paper proposes a new model for CT medical image de-noising, which is using independent component analysis and curvelet transform. Firstly, a random matrix was produce to separate the CT image into a separated image for estimate. Then curvelet transform was applied to optimize the coefficients. At last, the coefficients were selected for image reconstruction by inverse of the curvelet transform.

G.Y. Chen (2007) has presented novel image denoising method by incorporating the dual-tree complex wavelets into the ordinary ridgelet transform. The approximate shift invariant property of the dual-tree complex wavelet and the high directional sensitivity of the ridgelet transform make the new method a very good choice for image denoising. The author apply the digital complex ridgelet transform to denoise some standard images corrupted with additive white noise. Experimental results show that the new method outperforms VisuShrink, the ordinary ridgelet image denoising, and wiener2 filter both in terms of peak signal-to-noise ratio and in visual quality. In particular, the method preserves sharp edges better while removing white noise.

Mr. Devanand Bhonsle (2013) has presented the first model is developed with wavelet based thresholding algorithm. In this algorithm, the images are decomposed into four subbands. As most of the researchers have used db8 filters for image denoising, the same has been considered in this work too. Though lowering of the thresholding value below 0.01 yields better PSNR but the visual qualities of the denoised images are not as good as with the threshold value of 0.01.The image is denoised first with bilateral filter followed by decomposition into four subbands using db8 filters. In the next level the wavelet based soft thresholding is applied on all the subbands. The value of soft-thresholding is set at the same value obtained with wavelet thresholding only.

2.2 PAPERS RELATED TO REGION SEGMENTATION

David A. Clausi (2010) has presented a MRF (Markov Random Field) based multivariate segmentation algorithm named MIRGS (Multivariate Iterative Region Growing using Semantics), which extends the applicability of IRGS to multivariate images while inheriting the merits of IRGS (Iterative Region Growing using Semantics). To suppress initialization sensitivity, MIRGS uses a RKM (Region K level Means) based initialization method, which consistently provides accurate initial conditions at low computational cost. The superiority of RKM relative to two commonly used initialization schemes has been demonstrated on images with different feature space dimensions. For a variety of synthetic and natural multivariate images, MIRGS consistently achieves the highest segmentation accuracy compared to three other published algorithms.

Radha Chitta (2010) has presented two level k-means algorithm would be very useful for handling large datasets. A significant speedup is achieved in the clustering process. Analytical and empirical results also show that a good reduction in the computational complexity can be achieved while maintaining the same generalization performance by incorporating this algorithm in the training process of classifiers. There are many domains in which there is a requirement for algorithms which can handle large datasets. Some of the domains in which the proposed algorithm would prove to be useful are: i). Topic based web search, ii).Spam filtering, iii). Communication network analysis.

Jitedra Malik (2001) has developed a general algorithm for partitioning grayscale images into disjoint regions of coherent brightness and texture. The novel contribution of the work is in cue integration for image segmentation the cues of contour and texture differences are exploited simultaneously. Hence the experimental results as promising and hope that the paper will spark renewed research activity in image segmentation, one of the central problems of computer vision.

S.M.Ali (2013) has presented four different techniques have been implemented to extract and calculate the area of the tumor region for four successive slices of T2 weighted MR images. As it has been evidenced, the morphological method produced extensively different results than that fabricated by the adopted probabilistic calculation. The smoothing operation changed the results of the fuzzy C-means when fuzzy grouped with K-means. This behavior may be utilized to improve the classification accuracy as expected due to the dependency of K-mean method on the initial seeds. However more work may be required to improve the segmentation results, this may be achieved by implementin certain supervised classification method.

Anil K. Jain (2010) has presented the data clustering 50 years beyond K-means. The organizing data into sensible groupings is one of the most fundamental modes of understanding and learning. Clustering has a long and rich history in a variety of scientific fields.

2.3 PAPERS RELATED TO CLASSIFICATION

Hassan Khotanlou (2009) has presented this method is applicable to different types of tumors. First, the brain is segmented using a new approach, robust to the presence of tumors. Then first tumor detection is performed, based on selecting asymmetric areas with respect to the approximate brain symmetry plane and fuzzy classification. Its result constitutes the initialization of a segmentation method based on a combination of a deformable model and spatial relations, leading to a precise segmentation of the tumors. Imprecision and variability are taken into account at all levels, using appropriate fuzzy models. The results obtained on different types of tumors have been evaluated by comparison with manual segmentations.

Loay Kadom Abood (2013) has presented the Magnetic Resonance Images, T2 weighted modality, have been pre-processed by bilateral filter to reduce the noise and maintaining edges among the different tissues. Four different techniques with morphological operations have been applied to extract the tumor region. These were: Gray level stretching and Sobel edge detection, K-Means Clustering technique based on location and intensity, Fuzzy C-Means Clustering, and an Adapted K-Means clustering technique and Fuzzy C-Means technique. The area of the extracted tumor regions has been calculated. The present work showed that the four implemented techniques can successfully detect and extract the brain tumor and thereby help doctors in identifying tumor's size and region.

Shahram Mohanna (2011) has presented search algorithm is a recently developed meta-heuristic optimization algorithm, which is suitable for solving optimization problems. To enhance the accuracy and convergence rate of this algorithm, an improved cuckoo search algorithm is proposed in this paper. Normally, the parameters of the cuckoo search are kept constant. This may lead to decreasing the efficiency of the algorithm. To cope with this issue, a proper strategy for tuning the cuckoo search parameters is presented. Considering several well-known benchmark problems, numerical studies reveal that the proposed algorithm can find better solutions in comparison with the solutions obtained by the cuckoo search. Therefore, it is anticipated that the improved cuckoo search algorithm can successfully be applied to a wide range of optimization problems.

M. Rakesh (2012) has presented the image segmentation and detection of tumor objects in MRI using FCM Algorithm. In this work, FCM (Fuzzy C-means) algorithm is implemented using the data compression technique without including the weight factor in the cluster center upadation criterion which further speeds up the process besides yielding considerable segmentation efficiency, The modified FCM algorithm is used for clustering abnormal MR brain images from four tumor classes namely metastate, meningioma, glioma and astrocytoma. Textural features namely correlation, contrast and entropy are extracted from the images are used for the clustering algorithm. The segmented outputs are analyzed based on the segmentation efficiency and convergence rate. A comparative analysis is performed with the conventional FCM algorithm to show the superior nature in terms of convergence rate. Experimental results show promising results for the modified FCM algorithm.

Zafer Iscan (2010) has presented the detection of tumor in MR (Magnetic Resonance) brain images. The performance of the novel method is investigated on one phantom and 20 original MR brain images with tumor and 50 normal (healthy) MR brain images. Before the segmentation process, 2D CWT (Continuous Wavelet Transform) is applied to reveal the characteristics of tissues in MR head images. Then, each MR image is segmented into seven classes by using the ISNN (Incremental Supervised Neural Network) and the wavelet-bands. After the segmentation process, the head is extracted from the background by simply discarding the background pixels. Symmetry axis of the head in the MR image is determined by using moment properties. Asymmetry is analyzed by using the Zernike moments of each of six tissues segmented in the head: two vectors are individually formed for the left and right hand sides of the symmetry axis on the sagittal plane by using the Zernike moments of the segmented tissues in the head. Presence of asymmetry and the tumors are inquired by considering the distance between these two vectors.

CHAPTER-3

METHODOLOGY

3.1 WORK FLOW

The proposed approach of image denoising is experimented with the CT medical images and the result is evaluated with the PSNR. The obtained denoised image is then evaluated for the parameters sensitivity and accuracy for estimating the correctness of the image. CT image is denoised with bilateral filter followed by decomposition into four subbands using db8 filters. In the next level the wavelet based soft thresholding is applied on all the subbands. The value of soft-thresholding is set at the same value obtained with wavelet thresholding only. The results obtained after thresholding are then used to reconstruct the image. In the last level, again bilateral filter is applied to get the final denoised image.
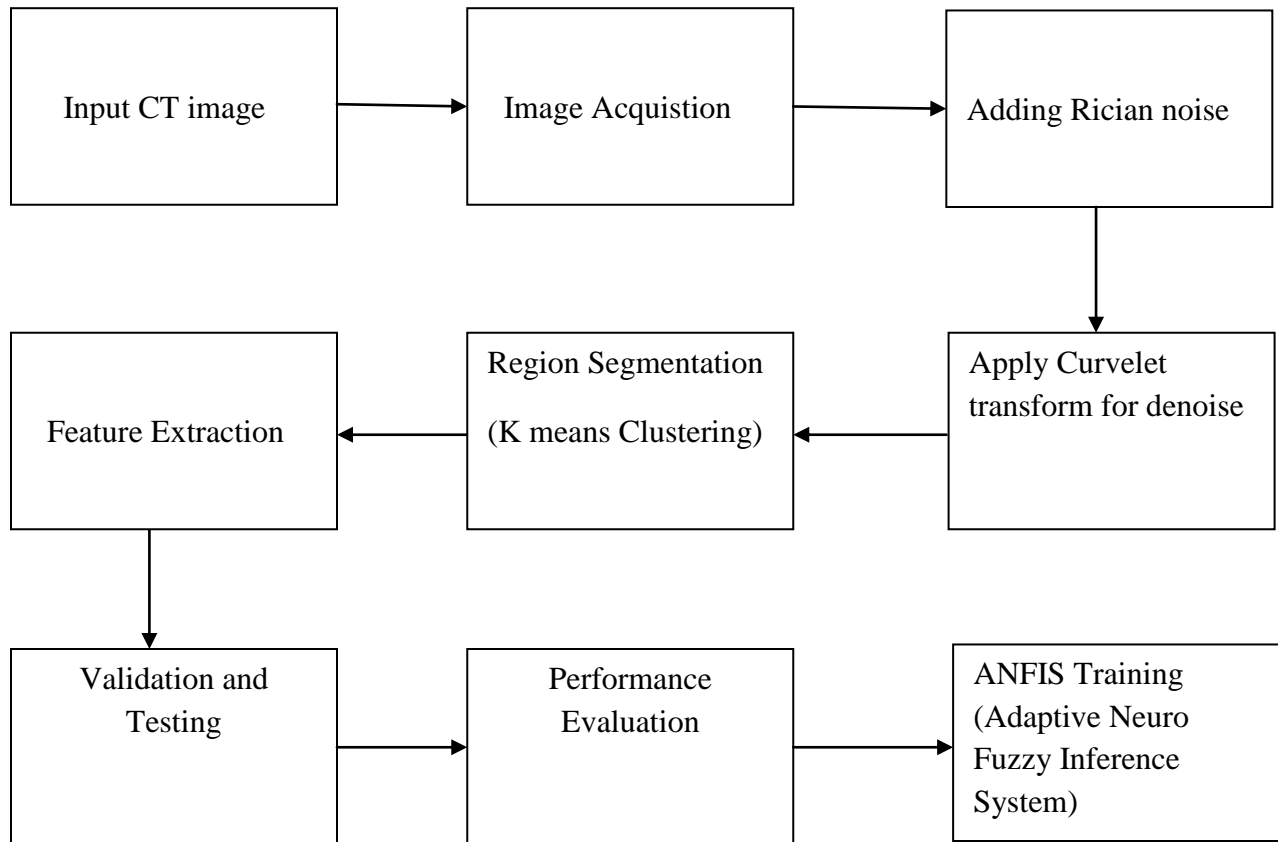
Fig 3.1 Work flow

3.2 STEPS INVOLVED METHODOLOGY

Step1: Read the input Image.

Step2: Resize the image.

Step3: Enhance the image using bilateral switching filter.

Step4: Add the Noise to the Enhanced image.

Step5: Apply Curvelet transform to denoise the noise from image.

Step6: Extract the Texture Features from the noise removed image using Grey level Co-occurrence Matrix.

Step7: Manual verification of Valid Features (Feature Selection).

Step8: Validating the System

Step 9: Testing the system

Step10: Performance Evaluation using PSNR.

Step11: Training the Features in Neuro Fuzzy System.

3.3 Image Acquistion

The first stage of any vision system is the image acquisition stage .After the image has been obtained, various methods of processing can be applied to the image to perform the many different vision tasks required today. However, if the image has not been acquired satisfactorily then the intended tasks should achievable, even with the aid of some form of image enhancement.

3.3.1. Energy

In order to capture an image a camera requires some sort of measurable energy. The energy of interest in this context is light or more generally electromagnetic waves. An electromagnetic (EM) wave can be described as massless entity, a photon, whose electric and magnetic fields vary sinusoidally, hence the name wave. The photon belongs to the group of fundamental particles and can be described in three different ways:

- A photon can be described by its energy E, which is measured in electron volts [eV].
- A photon can be described by its frequency f , which is measured in Hertz [Hz].
- A frequency is the number of cycles or wave-tops in one second
- A photon can be described by its wavelength λ, which is measured in meters [m].
- A wavelength is the distance between two wave-tops

The three different notations are connected through the speed of light c and Planck's constant h:

$$\lambda = \frac{c}{f}, \quad E = h \cdot f \Rightarrow E = \frac{h \cdot c}{\lambda}$$

3.3.2 Illumination

To capture an image, need some kind of energy source to illuminate the scene, the sun acts as the energy source. Most often apply visual light, but other frequencies can also be applied charge of the capturing process yourselves, it is of great importance to carefully think about how the scene should be lit. In fact, for the field of Machine Vision it is a rule-of-thumb that illumination is 2∕3 of the entire system design and software only 1∕3.

3.4 Image Denoising

Curvelets take the form of basis elements, which exhibit a very high directional sensitivity and are highly anisotropic. Curvelet transform is a newly developed mathematical transform is often used as time-frequency and multiresolution analysis tool in the signal and image processing domain. It combined the anisotropic of ridgelet with the multiscale characteristic of wavelet.

Actually the ridgelet transform is the core spirit of the curvelet transform. In 1999, an anisotropic geometric wavelet transform, named ridgelet transform, was proposed by Candes and Donoho. The ridgelet transform is optimal at representing straight-line singularities. Unfortunately, global straight-line singularities are rarely observed in ral applications. To analyze local line or curve singularities, a natural idea is to consider a partition of the image, and then to apply the ridgelet transform to the obtained sub-images. Apart from the blocking effect, however, the application of this so-called first generation curvelet transform is limited because the geometry of ridgelets is itself unclear, as they are not ture ridge functions in digital images. Later, a considerably simpler second-generation curvelet transform based on frequency partition technique was proposed. The second-generation curvelet transform has been shown to be a very efficient tool for many different applications in image processing. The overview of the curvelet transform is shown below by four step:
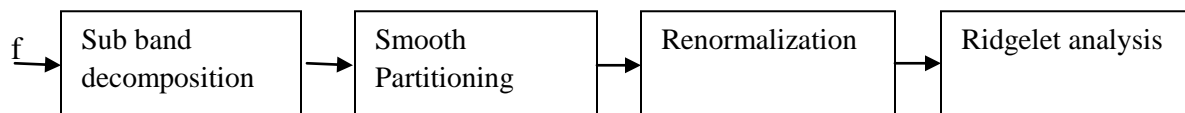
3.4.1 Curvelet transform

f → Sub band decomposition → Smooth Partitioning → Renormalization → Ridgelet analysis

Fig 3.4.1 Curvelet transform stages

3.4.2 Ridgelet Analysis

Before the Ridgelet Transform, there are some properties:

➤ The $\Delta_s f$ layer contains objects with frequencies near domain $|\xi| \in [2^{2s}, 2^{2s+2}]$.

➢ Windowing creates ridges of *width* $\approx 2^{-2s}$ and *length* $\approx 2^{-s}$

➢ The renormalized ridges has an aspect ratio of *width* $\approx$ *length*^{2}

Each 'square' is analyzed in the orthonormal ridgelet system. This is a system of basis element ρ_λ making an orthonomal basis for $L^2(\Re^2)$. There are some frequency domain analysis for Ridgelet below:
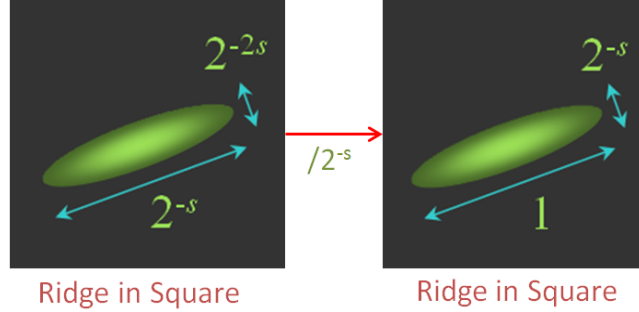

Fig 3.4.2 Ridgelet analysis

The ridgelet construction divides the frequency domain to dyadic coronae $|\xi| \in [2^s, 2^{s+1}]$. In the angular direction, it samples the s-th corona at least 2^s times. In the radial direction, it samples using local wavelets.

The ridgelet element has a formula in the frequency domain:

$$\hat{\rho}_\lambda(\xi) = \tfrac{1}{2}|\xi|^{-\frac{1}{2}}\left(\hat{\psi}_{j,k}\left(|\xi|\right)\cdot\omega_{i,l}(\theta) + \hat{\psi}_{j,k}\left(-|\xi|\right)\cdot\omega_{i,l}(\theta+\pi)\right)$$

➢ $\omega_{i,l}$: periodic wavelets for **[-π, π)**.
➢ i : the angular scale , $l \in [0, 2^{i-1}-1]$: the angular location.
➢ $\psi_{j,k}$: Meyer wavelets for $\Re$.
➢ j : the ridgelet scale , k : the ridgelet location.

Each normalized square is analyzed in the ridgelet system:

$$\alpha_{(Q,\lambda)} = \left\langle g_Q, \rho_\lambda \right\rangle$$

➢ The ridge fragment has an aspect ratio of $2^{-2s} \times 2^{-s}$.

➢ After the renormalization, it has localized frequency in band $|\xi| \in [2^s, 2^{s+1}]$.

➢ A ridge fragment needs only a very few ridgelet coefficients to represent it.
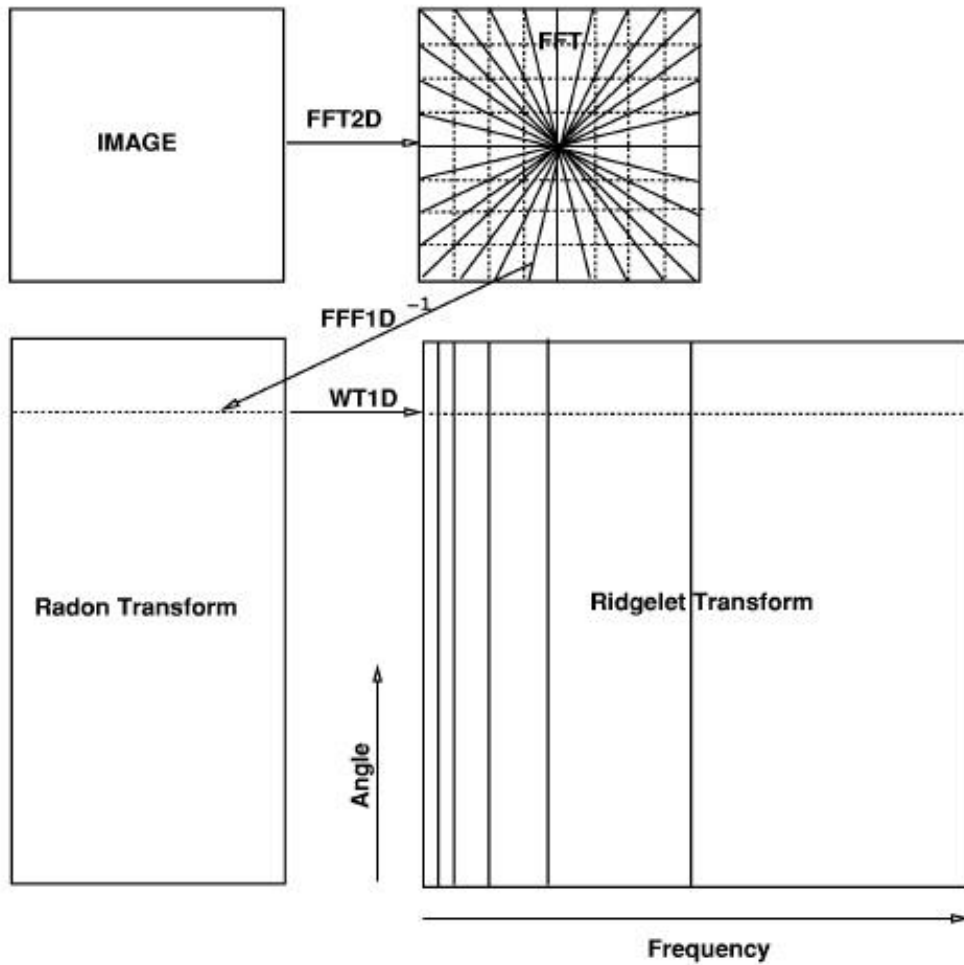
3.4.3 Ridgelet Transform

Fig 3.4.3 Ridgelet transform

3.4.4 Curvelet Transform stages

The idea of curvelets is to represent a curve as a superposition of functions of various lengths and widths obeying the scaling law width $\approx$ length^2. This can be done by first decomposing the image into subbands, i.e., separating the object into a series of disjoint scales. Each scale is then analyzed by means of a local ridgelet transform.

Curvelets are based on multiscale ridgelets combined with a spatial bandpass filtering operation to isolate different scales. This spatial bandpass filter nearly kills all multiscale ridgelets which are not in the frequency range of the filter. In other words, a curvelet is a multiscale ridgelet which lives in a prescribed frequency band. The bandpass is set so that the curvelet length and width at fine scales are related by a scaling law width $\approx$ length^2 and so the anisotropy increases with decreasing scale like a power law. There is a very special relationship between the depth of the multiscale pyramid and the index of the dyadic subbands; the side length of the localizing windows is doubled at every other dyadic subband, hence maintaining the fundamental property of the curvelet transform which says that elements of length about $2^{-j/2}$ serve for the analysis and synthesis of the subband $[2^j, 2^{j+1}]$.

While multiscale ridgelets have arbitrary dyadic length and arbitrary dyadic widths, curvelets have a scaling obeying width $\approx$ length^2. Loosely speaking, the curvelet dictionary is a subset of the multiscale ridgelet dictionary, but which allows reconstruction.

In opinion the "atrous" subband filtering algorithm is especially well-adapted to the needs of the digital curvelet transform. The algorithm decomposes an n by n image as a superposition of the form,

$$I(x, y) = c_j(x, y) + \sum_{j=1}^{J} w_j(x, y)$$

where, c_J coarse or smooth version of the original image and represents "the details of I" at scale for more information. Thus, the algorithm outputs J+1 subband arrays of size n x n. (The indexing is such that, here, j=1 corresponds to the finest scale, i.e., high frequencies.)

By following Curvelet transform opens us the possibility to analyse an image with different block sizes, but with a single transform. The idea is to first decompose the image into a set of wavelet bands, and to analyze each band by a ridgelet transform. The block size can be changed at each scale level.

The four stages are

(1). Sub band decomposition:

$$f \mapsto (P_0 f, \Delta_1 f, \Delta_2 f, \ldots)$$

P_0 - low pass filter

Δ_1, Δ_2 - Band pass filters

(2). Smooth partitioning:

$$h_Q = w_Q \cdot \Delta_s f$$

A grid of dyadic squares is defined as follows:

$$Q_{(s,k_1,k_2)} = \left[\frac{k_1}{2^s}, \frac{k_1+1}{2^s}\right] \times \left[\frac{k_2}{2^s}, \frac{k_2+1}{2^s}\right] \in \mathbf{Q}_s$$

$\mathbf{Q}s$ – all the dyadic squares of the grid.

w_Q is a displacement of w localized near Q.

(3). Renormalization:

$$(T_Q f)(x_1, x_2) = 2^s f\left(2^s x_1 - k_1, 2^s x_2 - k_2\right)$$

Each square is renormalized:

$$g_Q = T_Q^{-1} h_Q$$

(4). Ridgelet analysis:

$$\alpha_{(Q,\lambda)} = \langle g_Q, \rho_\lambda \rangle$$

The ridge fragment has an aspect ratio of $2^{-2s} \times 2^{-s}$.

After the renormalization, it has localized frequency in band $|\xi| \in [2^s, 2^{s+1}]$.

There is also procedural definition of the construction algorithm. The Inverse of the Curvelet Transform are given below:

(1) Ridgelet analysis:

$$g_Q = \sum_\lambda \alpha_{(Q,\lambda)} \cdot \rho_\lambda$$

(2) Renormalization:

$$h_Q = T_Q g_Q$$

(3) Smooth Integration:

$$\Delta_s f = \sum_{Q \in \mathbf{Q}_s} w_Q \cdot h_Q$$

(4) Sub-band Recomposition:

$$f = P_0(P_0 f) + \sum_s \Delta_s(\Delta_s f)$$

3.4.5 Curvelet Transform Construction
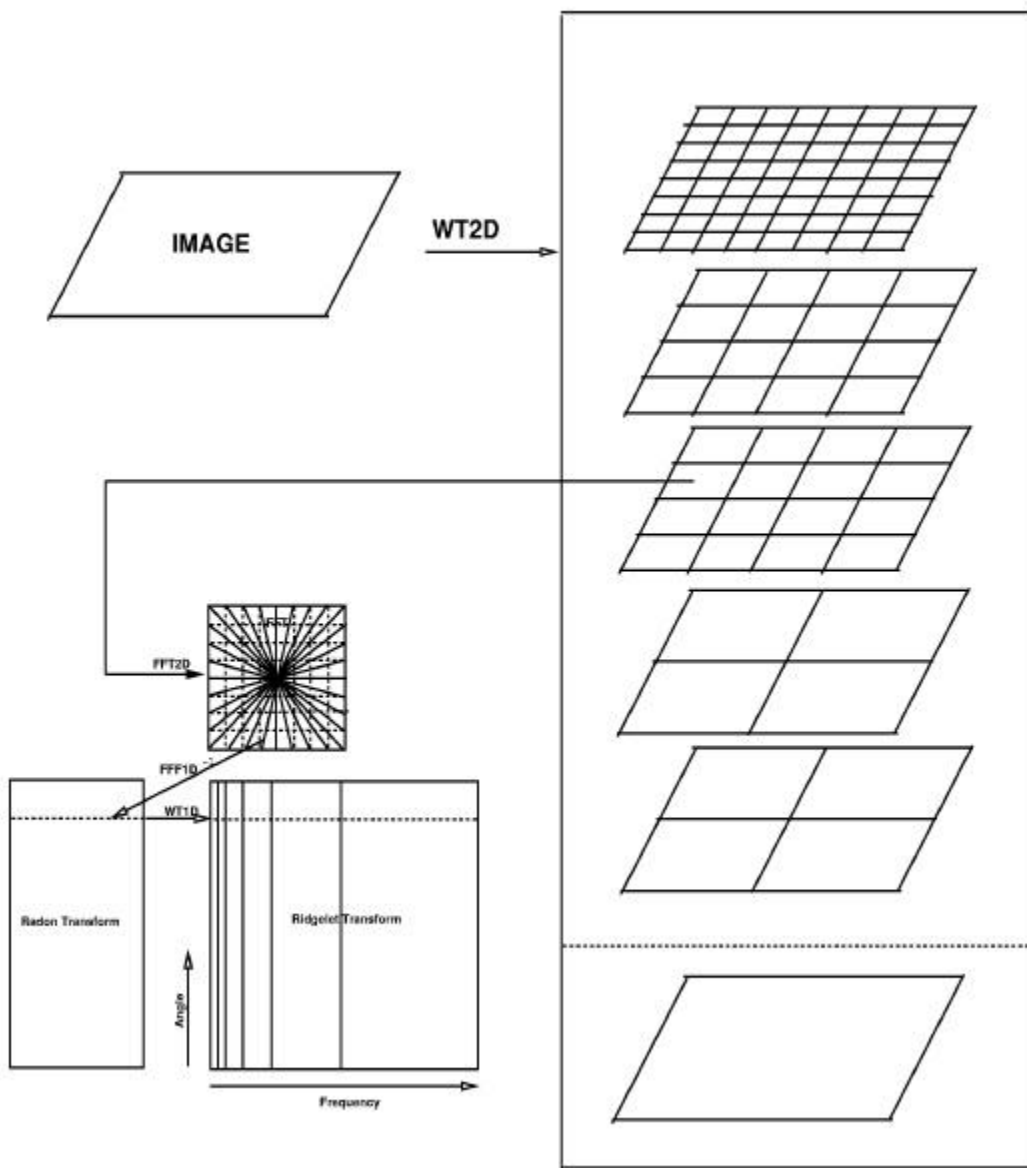
Fig 3.4.5 Curvelet transform

The above figure illustrates the decomposition of the original image into subbands followed by the spatial partitioning of each subband (i.e., each subband is decomposed into blocks). The ridgelet transform is then applied to each block.

This implementation of the curvelet transform is redundant. The redundancy factor is equal to 16J+1 whenever J scales are employed. Finally, the method enjoys exact reconstruction and stability, because each step of the transform is both invertible and stable.

3.5 Region Segmentation

Object detection and multi-class image segmentation are two closely related tasks that can be greatly improved when solved jointly by feeding information from one task to the other. However, current state-of-the-art models use a separate representation for each task making joint inference clumsy and leaving the classification of many parts of the scene ambiguous. In this work, use a hierarchical region-based approach to joint object detection and image segmentation.

This approach simultaneously reasons about pixels, regions and objects in a coherent probabilistic model. Pixel appearance features allow us to perform well on classifying amorphous background classes, while the explicit representation of regions facilitate the computation of more sophisticated features necessary for object detection. Importantly, this model gives a single unified description of the scene to explain every pixel in the image and enforce global consistency between all random variables.

3.5.1 Advantages

➢ Region Segmentation methods can correctly separate the regions that have the same properties should define.
➢ This method can provide the original images which have clear edges with good segmentation results.
➢ It can determine the seed points and the criteria want to make.
➢ Choose the multiple criteria at the same time.
➢ It performs well with respect to noise.

The Segmentation process is performed to extract the abnormal (tumours) portion of the brain from the brain MR image. This segmentation process make the segments of the brain MR image into two portions. One segment portion contains the brain tissues which are normal and

the second segment portion contains the tumorous cells. The segment part which contains the abnormal cells is the desired region which is known as tumors region.

After noise removal, K-Means clustering method was used to segment the image. This procedure illustrates the image using only the pixel intensity feature. To find the number of clusters accurately, K-Mean algorithm is iterated for a range of hypothesized numbers of clusters. Best choice for cluster is selected based on cluster validity measure. The silhouette validity method generated amazingly some good results for some of the test images.

3.5.2 K-means clustering

K-means clustering technique is used to partition the n data points into K classes . K-means clustering algorithm initially sets centroids of each cluster. regions are segmented from the denoised CT image by using K-means clustering algorithm. K-means clustering segments the concerned CT image into two specific regions. The former region consists of the normal cells whereas the second region is composed of the tumorous cells. K-means clustering segments the CT image based on the intensity of pixels constituting the image. K-means is one of the most significant unsupervised learning algorithms with respect to clusters. Clustering means, grouping of pixels based on their characteristics.

Here the image is clustered into k number of clusters. K-means clustering categorizes by minimizing the sum of squares of distances between data and the corresponding centroid of the cluster. Here, K-means clustering groups the pixels into two distinct clusters (k = 2).The detailed step-by steps of K-means clustering algorithm is presented as follows:
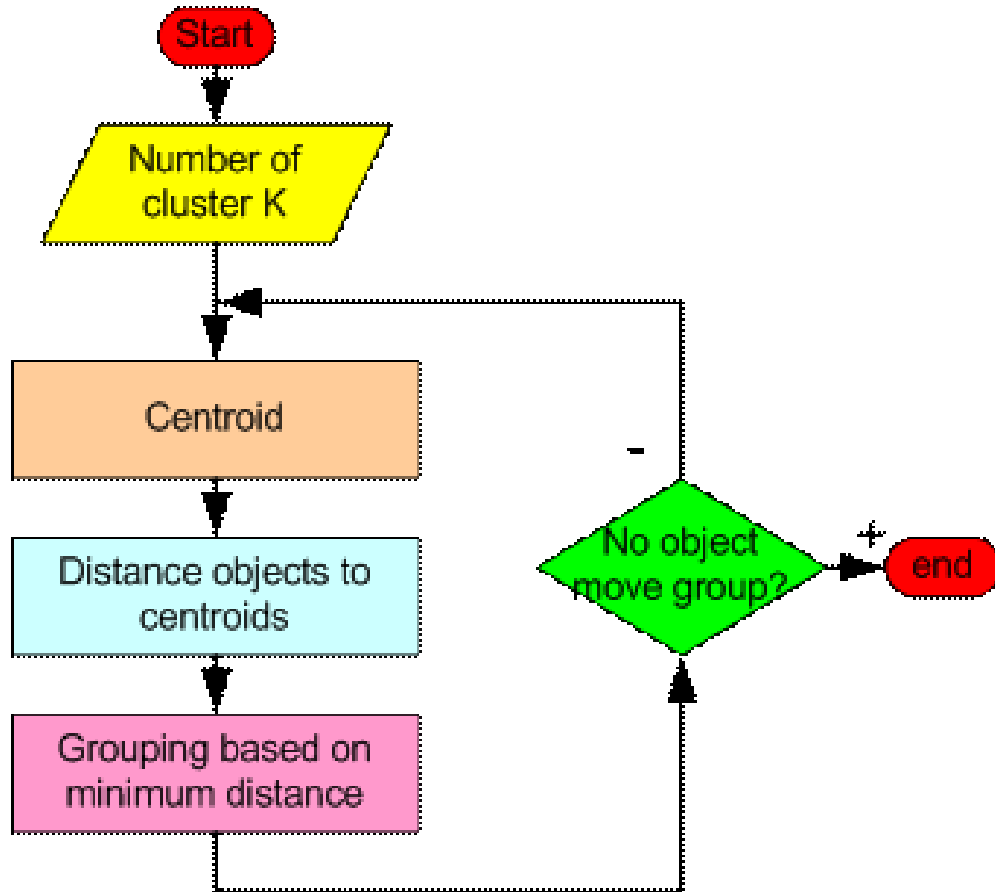
Fig 3.5.2 K means Clustering

1). Give the number of cluster value as k. Assume the value as k=2.

2). Randomly choose the k cluster centers.

3). Calculate mean or center of the cluster

$$M = \frac{\sum\limits_{i:c(i)=k} x_i}{N_k}, k = 1,2,..K$$

4). Next the pixels of the image are assigned to the closest cluster which satisfies the minimum Euclidean distance from the pixels values to center of each cluster.

$$D(i) = \arg\max \left\| x_i - M_k \right\|^2, I = 1,..K$$

5). If the distance is near to the center, then move to that cluster.

6). Else move to the next cluster

7). Re-estimate the center

8). Repeat the process until the center doesn't move further.

3.5.3 Cluster Validity

The Silhouette validation method calculates the silhouette width for each sample, average silhouette width for each cluster and overall average silhouette width for entire data set. By using this mechanism, each cluster could be represented by so-called silhouette, which is based on the evaluation of its compactness and separation. The average silhouette width could be applied for evaluation of clustering validity and also could be used to decide how good is the number of selected clusters, validity criteria is defined as

$$S(i) = \frac{(b(i) - a(i))}{\max\{a(i), b(i)\}}$$

where a(i) represents average dissimilarity of i-object to all other objects in the same cluster; b(i) represents minimum of average dissimilarity of i-object to all objects in other cluster (in the closest cluster).

If silhouette have the value nearly close to 1, it can be concluded that sample is "well-clustered" and it was assigned to a very appropriate cluster. If silhouette have the value near about zero, it can be concluded that, that sample of data could be dispense to another closest cluster as well, and the sample of that data chunk lies evenly far away from both clusters. If silhouette have the value nearly close to −1, it can be concluded that, sample is "misclassified" and is merely somewhere in between the clusters. The overall average silhouette width for the entire plot is simply the average of the S(i) for all objects in the whole dataset. The largest overall average silhouette indicates the best clustering (number of cluster). Therefore, the number of cluster with maximum overall average silhouette width is taken as the optimal number of the clusters.

3.6 Feature Extraction

Feature extraction defines the features of the given CT images, and their parameters. This phase should be denoted from the characteristics of an image to describe its texture properties. Graycoproperties calculates the statistics specified in properties from the gray-level co-occurrence matrix.

Graycoproperties normalizes the gray level co occurrence matrix (GLCM) so that the sum of its elements is equal to 1. It is the joint probability occurrence of pixel pairs with a defined spatial relationship having gray level values in the image.

Following are the properties defined as:

3.6.1 Contrast

Measure the intensity contrast between a pixel and its neighbor over the whole image.
Range = [size (GLCM, 1)-1 ^2]

$$\sum_{i,j} |i - j|^2 p(i, j) \qquad \text{... (1)}$$

3.6.2 Correlation

Measure of how correlated a pixel is to its neighbor over the whole image.
Range = [-1, 1]

$$\sum_{i,j} \frac{(i - \mu i)(j - \mu j) p(i, j)}{\sigma_i \, \sigma_j} \qquad \text{... (2)}$$

3.6.3 Energy

Returns the sum of squared elements in the GLCM.
Range = [0 1]

$$\sum_{i,j} p(i, j)^2 \qquad \text{... (3)}$$

3.6.4 Homogeneity

Returns a value that measures the closeness of the distribution of elements in the GLCM to the GLCM diagonal.

Homogeneity is 1 for a diagonal GLCM.

$$\sum_{i,j} \frac{p(i,j)}{1+|i-j|} \qquad \dots \quad (4)$$

3.7 Classification using Anfis Classifier

ANFIS is a fuzzy Sugeno model of integration where the final fuzzy inference system is optimized via the ANNs training. ANFIS can be viewed as a class of adaptive networks which are functionally equivalent to fuzzy inference system. It maps inputs through input membership function and associated parameters, and then through output membership function to outputs. ANFIS uses back-propagation or a combination of least square estimation and back-propagation for membership function parameter estimation. The most important point in data classification by ANFIS is designing of fuzzy rules. To solve this problem, several clustering techniques such as fuzzy c-means (FCM), K-means clustering (KMC) and histogram adaptive smoothing (HAS) can be utilized. In this study, subtractive clustering is used in which each cluster represents one independent rule.

3.7.1 Neuro Fuzzy Approach

Neuro Fuzzy is a hybrid of artificial neural networks and fuzzy logic.Neuro Fuzzy networks are the realizations of the functionality of fuzzy systems using neural techniques. Neuro Fuzzy Network incorporates the human-like reasoning style of fuzzy systems through the use of fuzzy sets and a linguistic model consisting of a set of IF-THEN rules as shown in Figure 3.7.1.
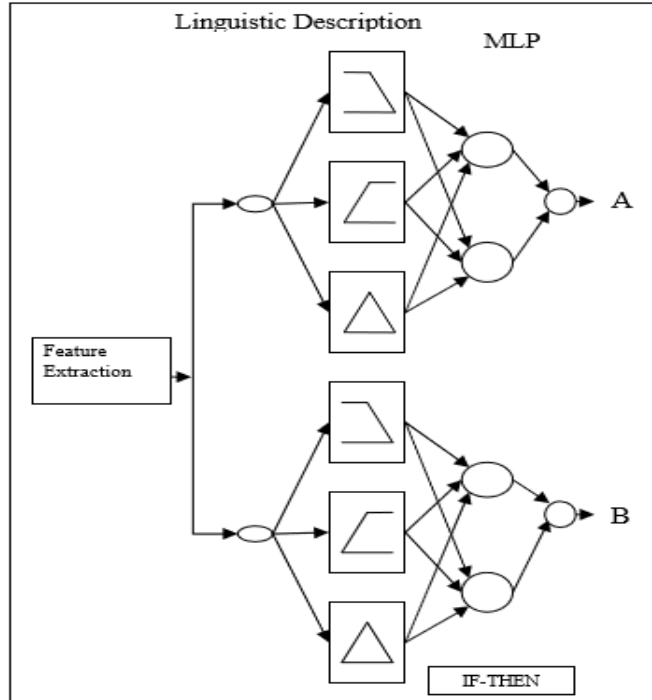
Figure 3.7.1 Structure of Feedforward Neuro Fuzzy

The important part of fuzzy layer, it is responsible to analyze the distribution of data and group the data into the different membership values. This membership value is applied as the input vector to the Multi- Layer Perceptron Neural Network classifier. The membership value also representing the parameter of each heart beat class.

In this project the output of DWT technique as feature vector and ANFIS as a Neuro Fuzzy Classifier for the ECG analysis is used, because the accuracy rates achieved by the combined neural network model presented for classification of the ECG beats is to be higher than the stand alone classifier model.

3.7.2 ANFIS Model

The ANFIS learning techniques provide a method for the fuzzy modeling procedure to learn information about data set, in order to compute the membership function parameters that best allow the associated fuzzy inference system to track the given input-output data. ANFIS constructs an input-output mapping based on both human knowledge (in the form of fuzzy if-

then rules) and simulated input output data pairs. It serves as a basis for building the set of fuzzy if then rules with appropriate membership functions to generate the input output pairs.
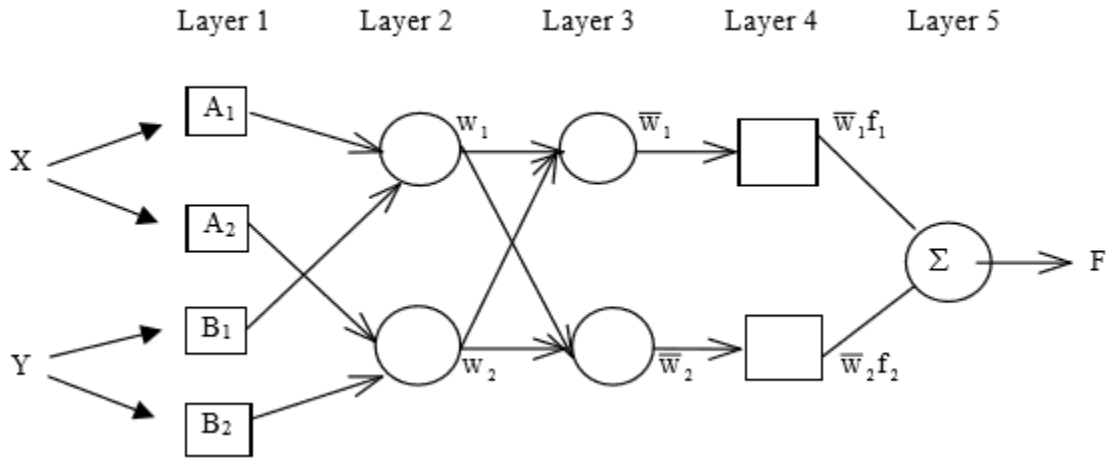
Figure 3.7.2 Basic structure of ANFIS model

ANFIS gives a powerful tool for data classification.

For example:

Rule 1: If x is A1 and y is B1 then f1=a1 x +b1 y + c1   (3)

Rule2: If x is A2 and y is B2 then f2 = a2 x +b2 y + c2   (4)

The nodes functions of ANFIS architecture are described below:

Layer 1: Every node I in this layer is a square node with a node function as in equation (5) and equation (6):

$$O_{1,i} = \mu_{Ai}(x), for\ I = 1,2 \tag{5}$$

$$O_{1,i} = \mu_{Bi-2}(y), for\ I = 3,4 \tag{6}$$

where x is the input to node I, and A_i (or $Bi - 1$) is a linguistic label (such as "small", "medium", "large") associated with this node. The $O_{1,i}$ is the membership function of a fuzzy set A_i and it specifies the degree to which the given input x satisfies the quantifier A_i. Usually chosen $\mu_{Ai}(x)$ to bell-shaped with maximum equal to 1 and minimum equal to 0, such as the generalized bell function in equation given by

$$\mu_{Ai}(x) = \frac{1}{1+\{(\frac{x-c_i}{a_i})^2\}^{bi}} \qquad (7)$$

where a_i, bi, ci is the parameter set.

Layer 2: Every node in this layer is a fixed node labels asπ, whose output is the product of all incoming signals defined by equation below,

$$O_{2,i} = w_i = \mu_{Ai}(x)\mu_{Bi}(y), \text{ for I=1, 2} \qquad (8)$$

Each node output represents the firing strength of a fuzzy rule.

Layer 3: Every node in this layer is a fixed node labelled N. The ith node calculates the ratio of the rule's firing strength to the sum of all rule's firing strengths as represent by equation below:

$$O_{3,i} = \bar{w}_i = \frac{w_i}{w_1+w_2}, \text{ for I=1,2} \qquad (9)$$

Outputs of this layer are called "normalized firing strengths".

Layer 4: Every node I in this layer is an adaptive node with a node function in equation below:

$$O_{4,i} = \bar{w}_i f_i = \bar{w}_i(p_i x + q_i y + r_i) \qquad (10)$$

where $\bar{w}_i$ is a normalized firing strength from layer 3 and (p_i, q_i, r_i) is the parameter set of this node. Parameters in this layer are referred to as "consequent parameters".

Layer 5: The single node in this layer is a fixed node labelled   that computes the overall output as the summation of all incoming signals in equation (11),

$$\text{Overall output}=O_{5,i}=\sum_i \bar{w}_i f_i=\frac{\sum_i \bar{w}_i f}{\sum_i \bar{w}_i} \qquad (11)$$

Thus an adaptive network, which is functionally equivalent to the Takagi- Sugeno type fuzzy inference system, has been constructed.

3.7.3 Grid Partitioning

ANFIS required a predefined network structure and its membership function as well as other parameters can be trained during the learning process. The system is first designed using Sugeno Fuzzy Inference System (FIS). There are two types of FIS namely Grid Partition and Subtractive Clustering.

The ANFIS Grid partition requires the number of membership functions for each input. This system uses the gbell shaped membership function to characterize the fuzzy sets input and Sugeno output membership functions as linear types. In the layer 1, there are four nodes have been used for each input dimension X_i where i=1,2 ..,d and d is the number of input dimensions.

The ANFIS which constructs a FIS, whose membership function parameters are tuned using a back-propagation algorithm in combination with a least squares type of method, which allows fuzzy systems to learn from the data that they are modeling.
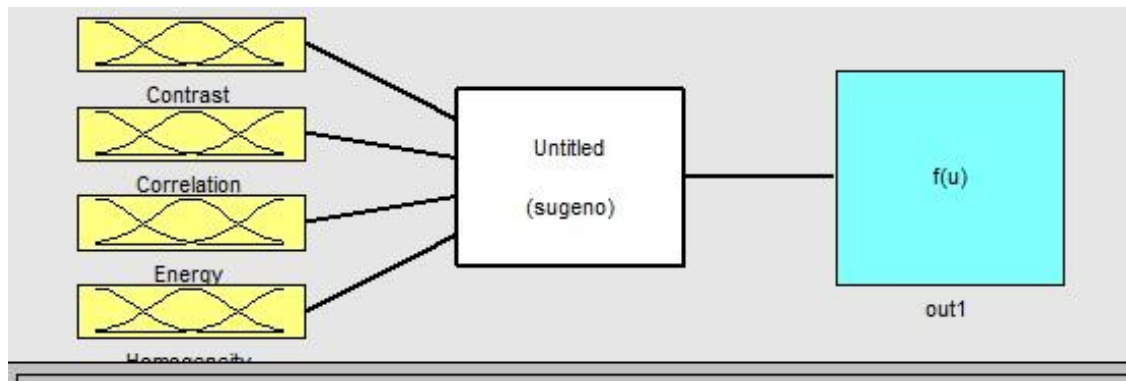
Figure 3.7.3(a) Fuzzy inference system for Brain Tumor classification
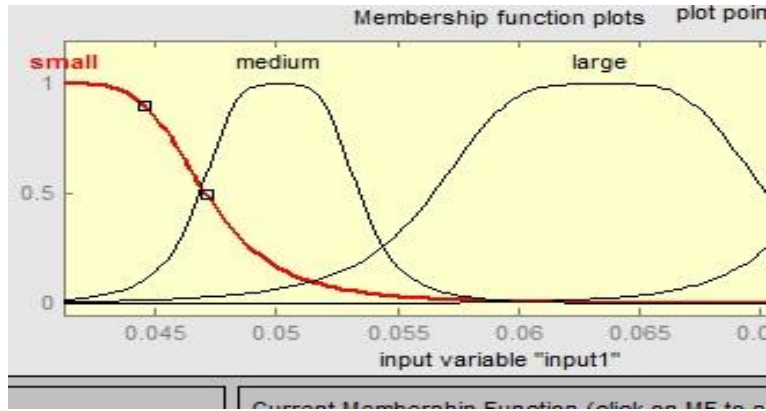
Figure 3.7.3(b) Initial membership functions

Based on the above Figure 3.7.3(b), the membership function of each input parameter was divided into three regions, which are small, medium and large. The examination of initial and final membership functions indicates that there are considerable changes in the final membership functions of the features.

3.7.4 Rule Base Identification

Based on the membership functions, then the fuzzy IF-THEN rules that have a fuzzy antecedent and constant consequence are constructed. The rule base is created according the expert knowledge using MATLAB rule base editor. Based on the three membership function (small, medium, large) that being used, the number of rule base created are given by

$$a^b = c \tag{12}$$

where,

a is membership function

b is number of input nodes

c is number of rules output

Therefore, for 3 membership functions and 4 input nodes,

a=3 membership functions, for small, medium, and large

b=4 input nodes, for contrast, correlation, energy, homogeneity.

a^ b=c

3^4= 81 rules are generated.

Rule	Contrast	Correlation	Energy	Homogeneity	Class
1	M	S	M	L	1
2	M	M	M	L	1
3	M	S	M	L	1
4	S	M	M	S	1
5	M	M	L	S	1
6	S	M	M	S	2
7	L	S	L	L	2
8	L	M	L	L	2
9	M	M	L	L	2
10	S	L	S	M	2

Table 3.7.4 Rules created by Expert knowledge

3.7.5 Subtractive Clustering

A Data clustering is a process of putting similar data into groups. A clustering algorithm partitions a data set into several groups such that the similarity within a group is larger than among groups. Clustering algorithms are used extensively not only to organize and categorize data, but are also useful for data compression and model construction. Clustering techniques are used in conjunction with radial basis function networks or fuzzy modeling primarily to determine initial location for radial basis functions or fuzzy if-then rules. There are different clustering technique such as k-means clustering, fuzzy c-means clustering, mountain clustering and

subtractive clustering. If there is no clear idea how many clusters there should be for a given set of data, subtractive clustering is a fast, one-pass algorithm for estimating the number of clusters and the cluster centers in a set of data. Consider a collection of n data points in an m-dimensional space. Without loss of generality, the data points are assumed to have been normalized within a hypercube. Since each data point is a candidate for cluster centers, a density measure at data point x_i is defined as:

$$D_j = \sum_{j=1}^{n} exp\left(\frac{-\left(\|x_i - x_j\|^2\right)}{\left(\frac{r_b}{2}\right)^2}\right) \qquad (13)$$

where r_a is a positive constant. Hence a data point will have a high density value if it has many neighboring data points. The radius r_a defines a neighbourhood; data points outside this radius contribute only slightly to the density measure. After the density measure of each data point has been calculated, the data point with the highest density measure is selected as the first cluster center. Let xc1 be the point selected and Dc1 its density measure. Next the density measure for each data point x_i is revised by the formula 2

$$D_i = D_{i-}D_{cl}exp\left(\frac{-\left(\|x_i - x_{cl}\|^2\right)}{\left(\frac{r_b}{2}\right)^2}\right) \qquad (14)$$

where r_b is a positive constant. Therefore, the data points near the first cluster center x_{c1} will have significantly reduced density measures, thereby making the points unlikely to be selected as the next cluster center. The constant r_b defines a neighborhood that has measurable reductions in density measure. The constant r_b is normally larger than ro to prevent closely spaced cluster centers; generally r_b is equal to 1.5 r_a. After the density measure for each data point is revised, the next cluster center x_{c2} is selected and all of the density measures for data points are revised again. This process is repeated until a sufficient number of cluster centers are generated. When applying subtractive clustering to a set of input-output data, each of the cluster centers represents a prototype that exhibits certain characteristics of the system to be modeled. These cluster centers would be reasonably used as the centers for the fuzzy rules premise in a zero-order Sugeno fuzzy model, or radial basis functions in a Radial Basis Function Network (RBFN). For instance, assume that the center for the i-th cluster is ci in an M dimension. The c_i can be decomposed into two component vectors p_i and q_i, where p_i is the input part and it

contains the first N element of c_i; q_i is the output part and it contains the last M - N elements of . Then given an input vector x, the degree to which fuzzy rule i is fulfilled is defined by

$$\mu_i = exp\left(\frac{-\left(\|x - x_p\|^2\right)}{\left(\frac{r_a}{2}\right)^2}\right) \tag{15}$$

This is also the definition of the i-th radial basis function by adopt the perspective of modeling using RBFNs. Once the premise part (or the radial basis functions) has been determined, the consequent part (or the weights for output unit in an RBFN) can be estimated by the least-squares method. After these procedures are completed, more accuracy can be gained by using gradient descent or other advanced derivative- based optimization schemes for further refinement.

For generating fuzzy inference system, the parameters of subtractive clustering are set as follow: Range of influence=0.5, Squash factor=0.55, Accept ratio=0.5, Reject ratio=0.15. With these parameters, 81 fuzzy rules are obtained. It should be noticed that several parameters such as types of activation functions and several values for NHLN, MEN, Range of influence, Squash factor ,Accept ratio and Reject ratio were examined and were altered based on trying-and-error method and suitable ranges and types were chosen for these parameters.

Subtractive clustering method finds cluster number of the specified input and it assigns membership functions equal to number of clusters. Gbell membership function is used and 81 rules are generated using 4 inputs, 1 output.

3.7.6 Advantages of the Sugeno Method:

- It is computationally efficient.
- It works well with linear techniques (e.g., PID control).
- It works well with optimization and adaptive techniques.
- It has guaranteed continuity of the output surface.
- It is well suited to mathematical analysis.

3.8 Peak Signal to Noise Ratio:

It defines the ratio between the maximum possible power of a signal and the power of corrupting noise that affects the fidelity of its representation. Because many signals have a very wide dynamic range, PSNR is usually expressed in terms of the logarithmic decibel scale.

PSNR is most commonly used to measure the quality of reconstruction of lossy compression codecs. The signal in this case is the original data, and the noise is the error introduced by compression.

When comparing compression codecs, PSNR is an approximation to human perception of reconstruction quality. Although a higher PSNR generally indicates that the reconstruction is of higher quality, in some cases it may not. One has to be extremely careful with the range of validity of this metric; it is only conclusively valid when it is used to compare results from the same codec (or codec type) and same content. PSNR is most easily defined via the mean squared error (MSE).

Given a noise-free m×n monochrome image I and its noisy approximation K, MSE is defined as,

The PSNR (in dB) is defined as:

$$PSNR = 10log_{10} \frac{E_{max}^2 \ X \ I_w \ X \ I_h}{\Sigma(I_{xy} - I_{xy}^*)}$$

where,

I_w and I_h = width and height of the denoised image

I_{xy} = Original image pixel value at coordinate (x, y)

I_{xy}^* = Denoised image pixel value at coordinate (x, y)

E_{max^2} = Largest energy of the image pixels.

CHAPTER-4

4. SIMULATION RESULTS

The Proposed method is implemented in a Windows machine having a configuration of Intel (R) core i5 processor, 2.40 Ghz, 4 GB RAM and the operation system platform is Microsoft Windows 7 Ultimate. This proposed technique has been implemented using MATLAB version (R2012). For denoising the CT images the Curvelet Toolbox has been used. The following phases such as Region Segmentation are implemented using K-means Clustering Toolbox and Classification is evaluated by using ANFIS Toolbox.

PROCEDURE

4.1 Image Denoising

Normally CT image has noise present in nature, in this project denoise the given image by using Curvelet Transform stages. The four stages are Sub band decomposition, Smooth Partitioning, Renormalization and Ridgelet Analysis. Initially the noise in the CT image applying the wavelet in 2dimensional with respect to six subbands with low pass and Band pass filters. It separates the image into Partitioning, within these take one subband and applying Fast fourier transform in 2 dimensional for separating the radial lines with the scaling law of width $\approx$ length^2. Renormalization has changing the ridge fragment 2^{-2s}x 2^{-s} into $|\xi| \in \left[2^s, 2^{s+1}\right]$. By following with an radial line fast fourier transform in 1 dimensional are applied then get the initial Radon transform. With these transform take wavelet in 1 dimensional for the construction of Ridgelet transform. By using the polar coordinates the denoising process is done with the reconstruction of inverse of the Curvelet Transform.

Given below images represents the procedural steps of outputs for denoise:
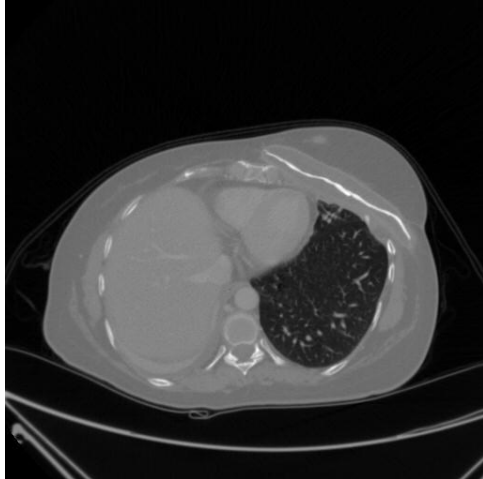
Fig 4.1(a) CT image
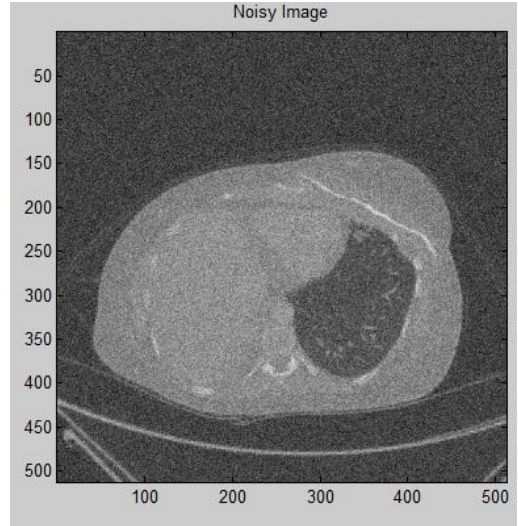
Fig 4.1(b) Noisy image
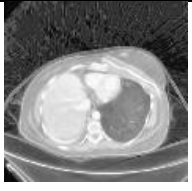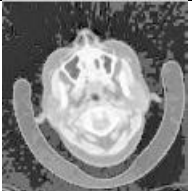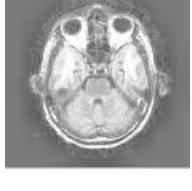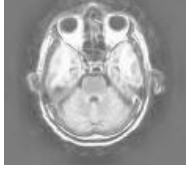
Each CT image has chosen for classification is stored in a database. It has the resolution of 512 x 512 and is available in standard JPEG format. Since most of the real time images have signal dependent noise it is suitable to add Rician noise to the available database before denoising.

4.1.1 Denoising Results with Curvelet Transform

Fig 4.1.1(a) Denoised CT image

According to Literature survey, it has been found that there are various transforms to remove noise from images. Out of the various transforms it has been found that Dual Tree Complex Wavelet Packet Transform and Curvelet Transform has good results of removing noise in CT images. When comparing the PSNR values obtained from Dual Tree Complex Wavelet Transform with the results obtained from Curvelet Transform it has shown that there is a significant improvement in PSNR values in the proposed method. It has been found that the execution time for Curvelet transform denoising process is 4.135ms which is very fast compared to the execution time required for Dual Tree Complex Wavelet Transform.

Input CT image	Output CT image	PSNR values get by Curvelet transform	PSNR values get by Dual Tree Complex Wavelet Packet Transform
		26.2979	21.634
		25.9171	18.918
		26.2787	21.730
		25.8248	21.889
		28.6812	18.988
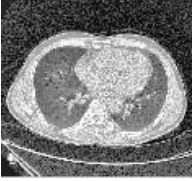
		29.0536	21.463

Table 4.1.1(b) Showing the denoising results (PSNR in dB) with Curvelet Transform

The PSNR values obtained for the 6 sample images of the database has been tabulated in Table 4.2.5 with the values of PSNR of Dual Tree Complex Wavelet Packet Transform marked against each image as proposed by A.Velayudham et. al.

4.2 Region Segmentation

Region Segmentation is done by using K-means Clustering Algorithm. K-means Clustering segments the concerned CT image into two specific regions such as normal cells and tumorous cells. Clustering defines the grouping of pixels based on their characteristics.

K-means Clustering categorizes the image into clusters by minimizing the sum of squares of distances between data and the corresponding centroid of the cluster.

4.2.1 Cluster image
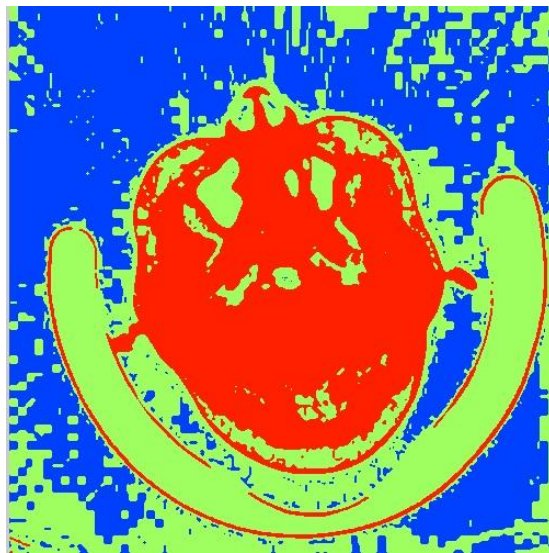
Fig 4.2.1 Cluster formation

The above figure describes the Cluster formation by segmenting the image into clusters based on intensity of the pixels constituting the image.

4.2.2 Segmentation Output
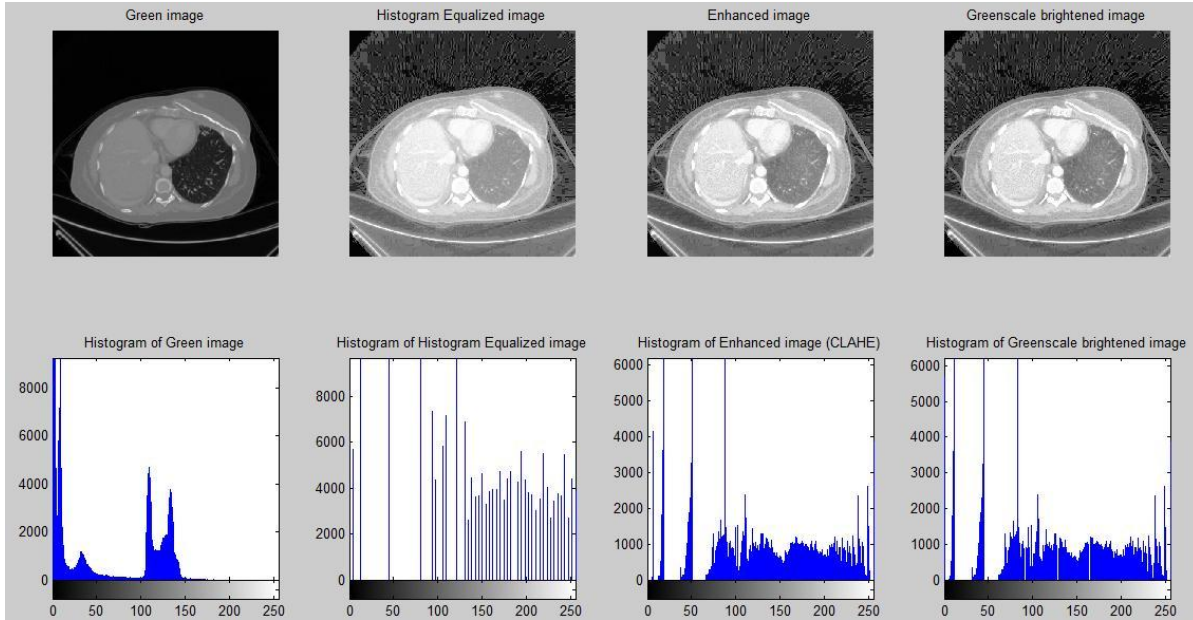
Fig 4.2.2 CT image result of Segmentation

Fig 4.2.2 represents the CT image segmentation by denoting the Green image, Histogram Equalized image, Enhanced image and Greenscale brightened image. Histogram is a graphical representation of the distribution of data. It is an estimate of the probability distribution a continuous variable. Here the missing internal part of the human brain is identified by histogram. For biomedical information representing the Green component image with histogram equalization. Enhancement of the image is carried out using Contrast Limited Adaptive Histogram Equalization (CLAHE). It operates on small regions in the image called tiles, rather than the entire image. Each tile's contrast is enhanced, so that the histogram of the output region approximately matches the histogram specified by the Distribution parameter. The neighboring tiles are then combined using bilinear interpolation to eliminate artificially induced boundaries. The contrast especially in homogeneous areas can be limited to avoid amplifying any noise that might be present in the image.

41

4.3 Feature Extraction

Feature Extraction is carried out by using Gray Level Co-occurrence Matrix of having Graycoproperties. For classifying the CT image the following features such as Contrast, Correlation, Energy and Homogeneity are extracted by using the Graycoproperties. Upon execution of the feature extraction program in MATLAB, the obtained results for contrast, correlation, energy and homogeneity features are tabulated in table 4.3
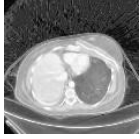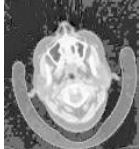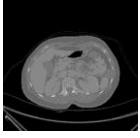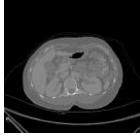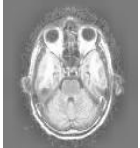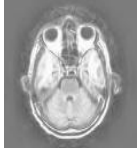
Input CT image	Output CT image	Contrast	Correlation	Energy	Homogeneity
		0.052	0.990	0.376	0.975
		0.041	0.990	0.516	0.980
		0.0409	0.9921	0.4592	0.9805
		0.055	0.989	0.515	0.973
		0.083	0.975	0.490	0.963
		0.077	0.982	0.452	0.962

Table 4.3 Feature Extraction Output

4.4 Classification using ANFIS:

Adaptive Neuro Fuzzy Inference System Classifier provides a clear view about the diagnosis of the given CT image. The four input parameters obtained from feature extraction are used to form the membership functions and finally provide a defuzzification output. The inputs to the ANFIS Classifier are the feature extraction values obtained from the previous module which are used in training the data. The output from previous stage is stored in the workspace in Excel format which is loaded as input to the classifier.

The given below diagram describes the loading of data to the ANFIS classifier of the ANFIS classification tool box which is provide as input to the next stage. The generation of FIS structure and training the FIS structure for the feature values are carried out further.

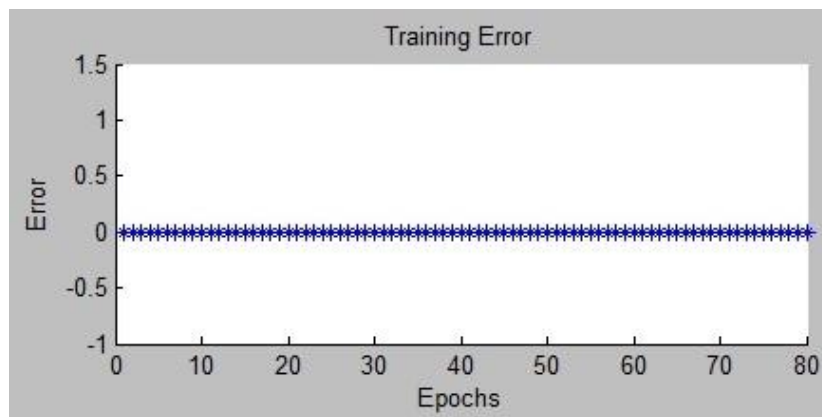**Fig 4.4.1 Training the data**

Fig 4.4.2 ANFIS network error

Based on the figure 4.4.2, the ANFIS used 500 data in 80 training periods and the step size for parameter adaptation had an initial value of 0.001. At the end of 80 training periods, the network error convergence curve of ANFIS had the final error convergence value which is 0.00044255.

Figure 4.4.3 Training data

The Figure 4.4.3 shows that the ANFIS output in asterisk marks are correctly classified into four classes.
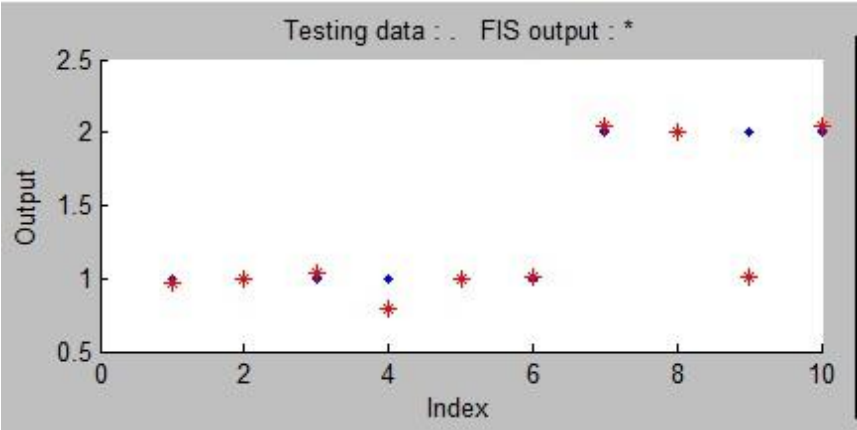

Figure 4.4.4 Testing data

The Figure 4.4.4 shows the testing data, where the asterisk marks are the output of ANFIS classifier, that starts to overfit with the target classes.
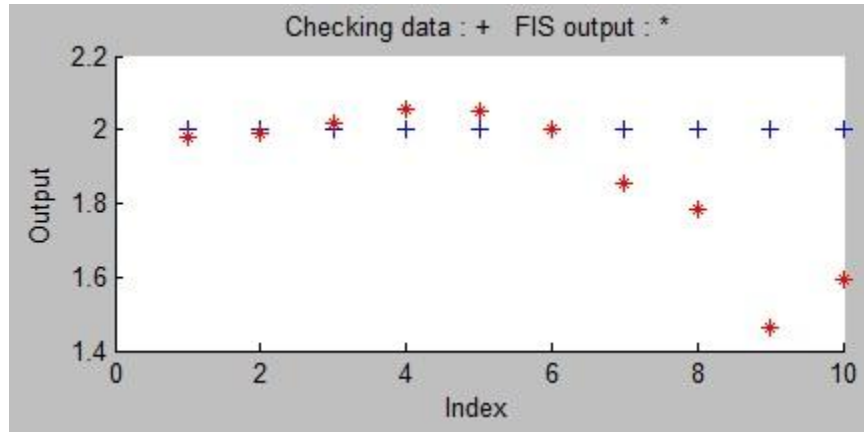
44

Figure 4.4.5 Checking data

The Figure 4.4.5 shows the checking data validation model, that overfits with training output.

Figure 4.4.6 Training data using subtractive clustering

The subtractive clustering technique, generates clusters and depending on the cluster calculates the number of membership functions. Figure 4.4.6 shows the target of classes 1,2,3,4 and the ANFIS output. A set of 10 datas are taken for testing and tested using subtractive clustering.
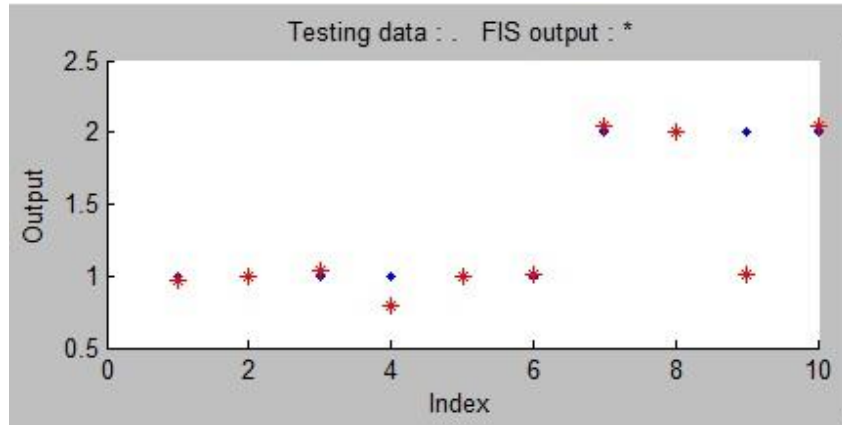
45

Figure 4.4.7 Testing data using subtractive clustering

The four statistical features are selected and three membership functions are formulated. The three membership functions are named small, medium and large. The membership funcions before training are shown below in Figure 4.4.7 (a),(b),(c),(d).
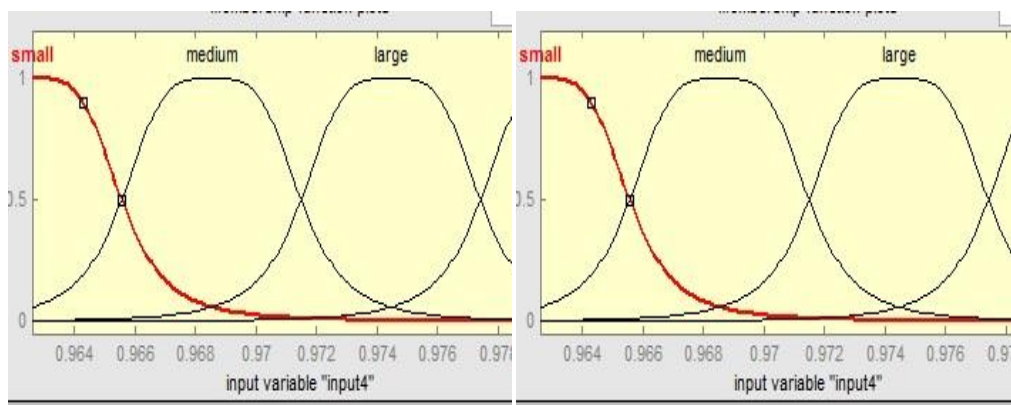

Figure 4.4.7 (a)Contrast

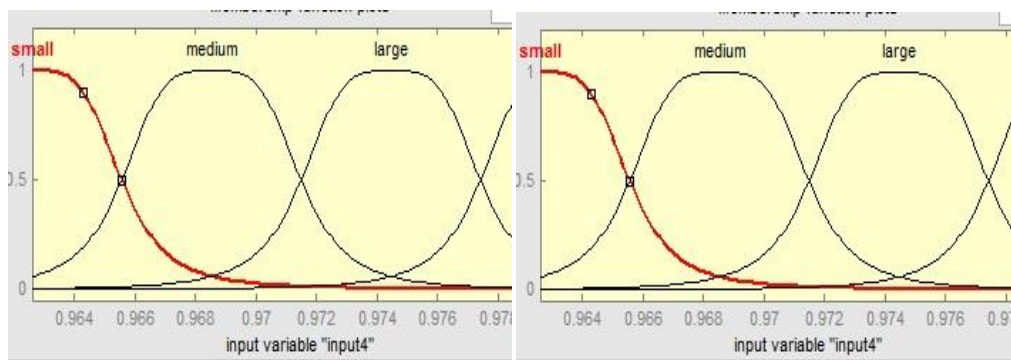**Figure 4.4.7 (b) Correlation**

Figure 4.4.7 (c) Energy

Figure 4.4.7 (d) Homogeneity

The classification of the features using grid partitioning is shown below which is carried out in the generate FIS block.
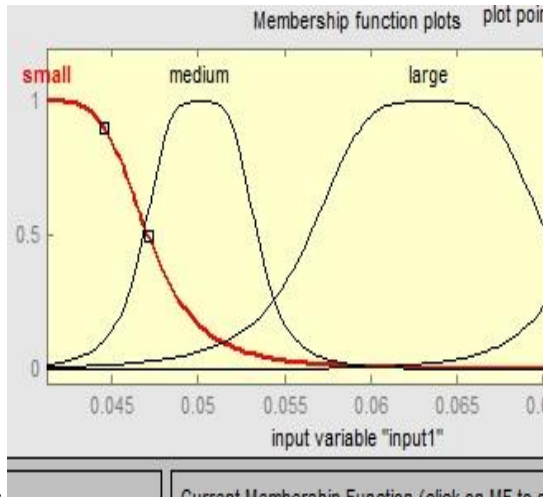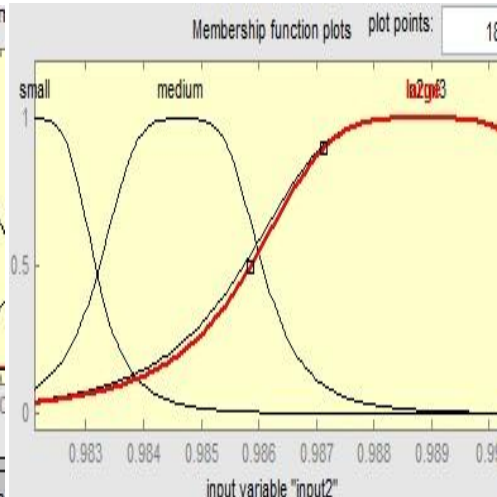

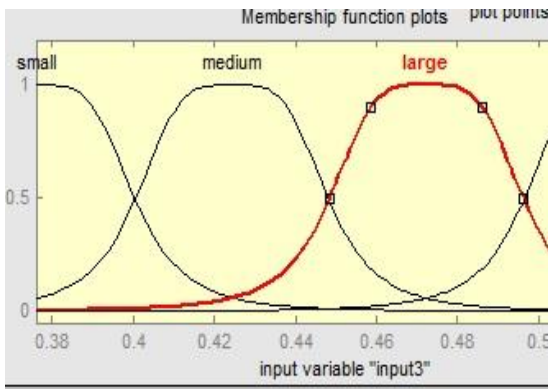**Figure 4.4.7(a) Contrast coefficients**   **Figure 4.4.7(b) Correlation coefficients**
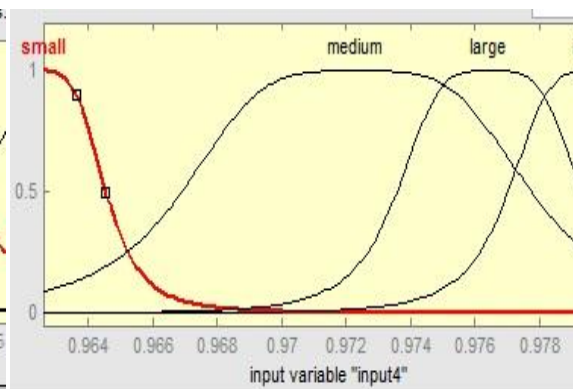

Figure 4.4.7(c) Energy coefficients   **Figure 4.4.7 (d) Homogeneity coefficients**
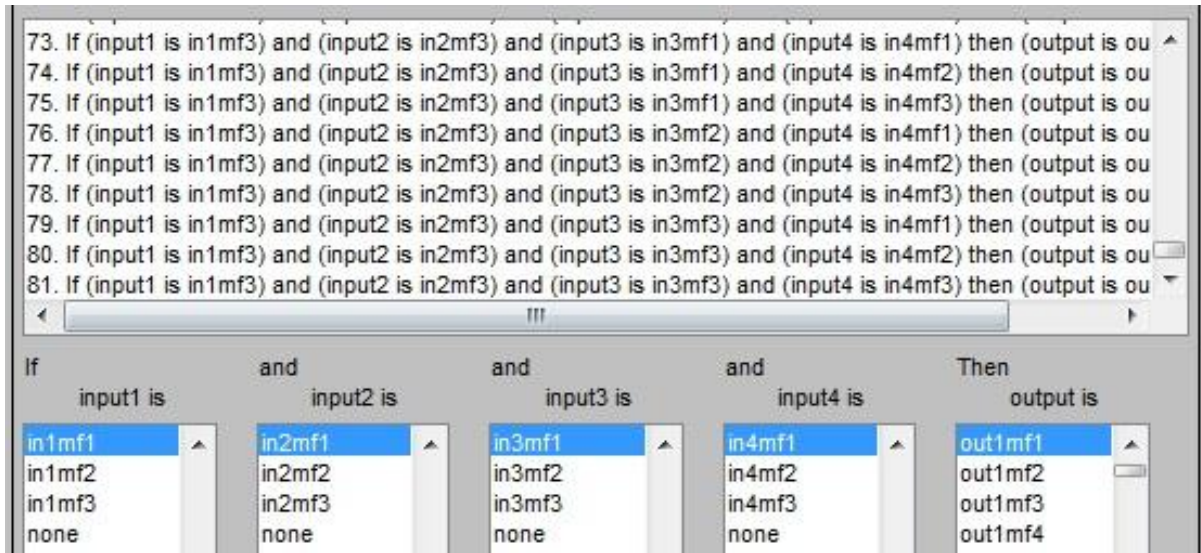
Figure 4.4.8 Rules generated using grid partitioning

These are the 81 rules generated using Grid partitioning method of ANFIS classifier. There are four inputs and single output. The final output is the weighted average of each rule's input.
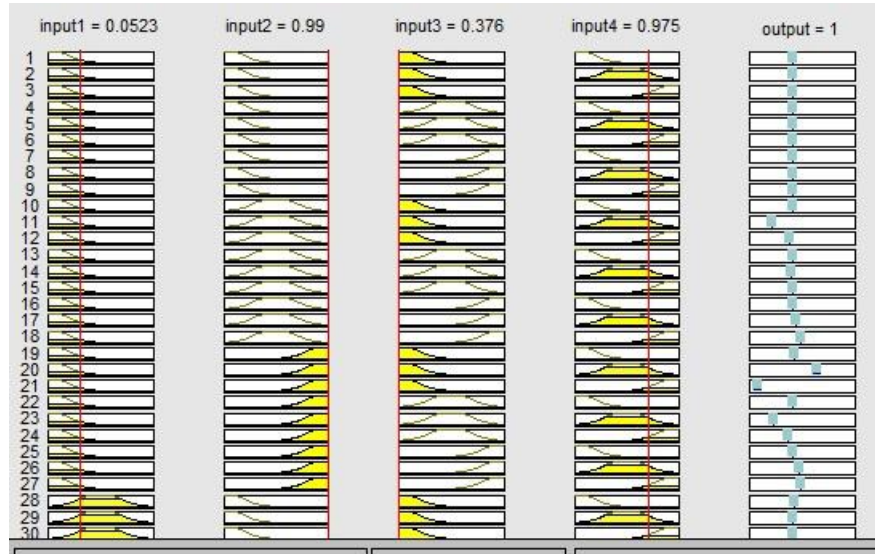

Fig 4.4.9(a) Rules generated result of classification

The above figure 5.2 defines the rule generation with the defuzzified output with class 1. The given data can be classified with the four membership functions and show it the output classification as normal condition. Hence it denotes the training and testing datas are gave the normal results.
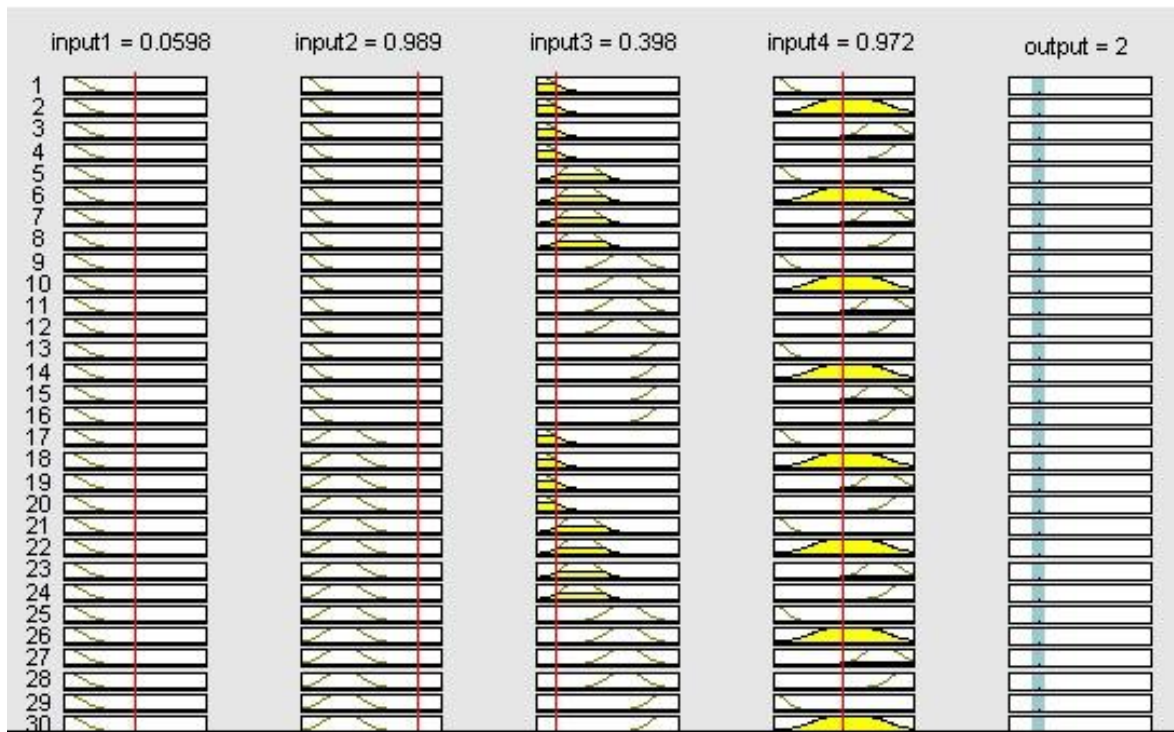
Fig 4.4.9(b) Rules generated for abnormal condition

With the following rules are generated, the given class values are calculated and classification of having normal or abnormal CT image is performed in the final stage. Therefore, the given class value is classified and show the target output as brain tumour image.

CHAPTER -5

CONCLUSION AND FUTURE WORK

The above calculations are being performed on an image of resolution 512×512 and work is being done to remove Rician noise of the images and future plan is to make it valuable for different resolution and for different size of images. In the denoising phase Curvelet Transform is used for removing noise. In the segmentation process K-means clustering technique is employed. In classification, a modified technique called Adaptive Neuro Fuzzy Inference System (ANFIS) algorithm is developed and applied for detection of the tumour region. From the obtained outcomes, it can conclude that the proposed denoising technique have shown better values for the PSNR of 29.0536. The ANFIS algorithm is employed for training the neural network and the fuzzy rules are generated according to the weights of the training sets and diagnosis of CT images for brain tumour is performed. This classification is done based on the fuzzy rules generated. The Performance of the ANFIS Classifier can be improved by weight optimization with the help of advanced optimization techniques in the future.

REFERENCES

1. Mr.Devanand Bhonsle, Nidhi Chandrakar, " A New Hybrid Denoising Method", Journal of Engineering, Computers & Applied Sciences (JEC&AS) Volume 2 No.1, January(2013).

2. Anja Borsdorf, Rainer Raupach, Thomas Flohr, "Wavelet Based Noise Reduction in CT images using Correlation Analysis", IEEE Transactions on Medical Imaging, Vol.27, NO.12, December (2008).

3. Jean-Luc Starck, Fionn Murtagh. Emmanuel J.Candes, "Gray and Color Image Contrast Enhancement by the Curvelet Transform", IEEE Transactions on Image Processing,Vol.12, NO.6, June(2003).

4. Tao Wang, Irene Cheng, Anup Basu "Fluid Vector Flow and Applications in Brain Tumor Segmentation", IEEE Transactions on Biomedical Engineering, Vol. 56, No. 3, March (2009).

5. Norden E.Huang, Zheng Shen R.Long, "The empirical mode decomposition and the Hilbert spectrum for nonlinear an Non-stationary time series analysis", The Royal Society(1998).

6. S.M.Ali, Loay Kadom Abood, Rabab Saadoon Abdoon, "Brain Tumor Extraction in MRI images using Clustering and Morphological Operations Techniques", International Journal of Geographical Information System Applications, June (2013).

7. Guangming Zhang, Zhiming Cuil, "CT image Denoising Model Based on Independent Component Analysis and Curvelet Transform", Journal of Sofware, Vol.5, September (2010).

8. Ehsan Valian, Shahram Mohanna, "Improved Cuckoo Search Algorithm or Global Optimization", International Journal of Communications and Information Technology, IJCIT June (2011).

9. A.K. Qin, David A.Clausi, "Multivariate Image Segmentation using Semantic Region Growing with Adaptive Edge Penalty", IEEE Transactions on Image Processing, Vol.19, No.8, August (2010).

10. Zafer Iscan, Ziimray Dokur, "Tumor detection by using Zernike moments in segmented magnetic resonance brain images", Expert Systems with Applications 37 April (2010).

11. Minakshi Sharma, Dr.Sourabh Mukharjee, "Brain Tumor Segmentation using hybrid Genetic Algorithm and Artificial Neural Network Fuzzy Inference System (ANFIS)", International Journal of Fuzzy Logic System (IJFLS) Vol.2,No.4, October (2012).

12. Emmanuel J.Candes, David L.Donoho, "Curvelets- A Surprisingly Effective Nonadaptive Representation for objects with Edges", Saint-Malo Proceedings, (1999).

13. G.Y.Chen, B.Kegl, "Image denoising with complex ridgelets", Pattern Recognition 40 (2007).

14. Shanshan Wang, Yong Xia. "Gabor feature based nonlocal means filter for textured image denoising", J.Vis.Commun. Image R.23 (2012).

15. Jitendra Malik, Serge Belongie, "Contour and Texture Analysis for Image Segmentation", International Journal of Computer Vision 43(1), (2001).

16. Radha Chitta, M.Narasimha Murty, "Two level k-means clustering algorithm for k-τ relationship establishment and linear classification", Pattern Recognition 43 (2010).

17. Joao M. Sanches, Jacinto C. Nascimento and Jorge S. Marques, "Medical Image Noise Reduction using the Sylvester-Lyapunov Equation", IEEE Transactions on Image Processing, Vol. 17, No.9, September (2008).

18. M. Rakesh,T. Rav, "Image Segmentation and Detection of Tumor objects in MR Brain images using Fuzzy C-Means (FCM) Algorithm", International Journal of Engineering Research and Applications, vol.2, no.3,pp.2088-2094, (2012).

19. A.K. Jain, "Data clustering: 50 years beyond **K**-means", Pattern Recognition Letters, vol.31, no.8,pp. 651-666, (2010).

20. X.-S. yang, S. Deb, "Cuckoo search via Levy flights", in: Proc. of World Congress on Nature & Biologically Inspired Computing (NaBIC2009), December (2009), India.

21. V Naga Prudhvi Raj. Dr T Venkateswarlu, "Denoising of medical images using dual tree complex wavelet transform", Procedia Technology, Vol.4,pp.238-244, (2012).

22. Ehsan Nadernejad, Mohsen Nikpour, "Image denoising using new pixon representation based on fuzzy filtering and partial differential equations", Digital Signal Processing, Vol.22, pp.913-922, (2012).

23. Sachin D, Ruikar and Dharmpal D Doye, "Wavelet Based Image Denoising Technique", International Journal of Advanced Computer Science and Applications, Vol.2, No.3, p.49-53, (2011).

24. Karen Panetta, Yicong Zhou, Sos Agaian, and Hongwei Jia, "Nonlinear Unsharp Masking for Mammogram Enhancement", IEEE Transactions on Information Technology in Biomedicine, Vol. 15, No.6, November (2011).

25. Shutao Li, Leyuan Fang and Haitao Yin, "An Efficient Dictionary Learning Algorithm and its application to 3D Medical Image Denoising", IEEE Transactions on Biomedical Engineering, Vol.59, No.2, February (2012).

26. Syed Amjad Ali, Srinivasan Vathsal, K. Lal kishore, "An Efficient Denoising Tecnique for CT images using Window-based Multi-Wavelet Transformation and Thresholding", European Journal of Scientific Research, Vol.48, No.2, pp.315-325, (2010).

CONFERENCES AND PUBLICATIONS

❖ Presented a Paper entitled **"Classification of CT Image with Curvelet Transform using Denoise, Region Segmentation and Feature Extraction"** in the One day National Conference on Innovations in Signal Processing, Embedded Systems and Communication Technology (SPECT '15) held during 27th March 2015 at Kumaraguru College of Technology Campus, Coimbatore.